5-2018

The Incorporation of Graphene to Lithium Cobalt Oxide as a Cathode to Improve the Performance of Lithium Ion Batteries

Kenan Wang
University of Arkansas, Fayetteville

The Incorporation of Graphene to Lithium Cobalt Oxide as a Cathode to Improve the Performance of Lithium Ion Batteries

A thesis submitted in partial fulfillment
of the requirements for the degree of
Master of Science in Microelectronics-Photonics

by

Kenan Wang
Changchun University of Science and Technology
Bachelor of Science in Physics, 2011

May 2018
University of Arkansas

This thesis is approved for recommendation to the Graduate Council.

Simon S. Ang, Ph.D
Thesis Director

Ryan Tian, Ph.D
Committee Member

Yue Zhao, Ph.D
Committee Member

Rick Wise, Ph.D
Ex-officio Member

The following signatories attest that all software used in this thesis was legally licensed for use by Kenan Wang for research purposes and publication.

Mr. Kenan Wang, Student	Dr. Simon S. Ang, Thesis Director

This thesis was submitted to http://www.turnitin.com for plagiarism review by the TurnItIn company's software. The signatories have examined the report on this thesis that was returned by TurnItIn and attest that, in their opinion, the items highlighted by the software are incidental to common usage and are not plagiarized material.

Dr. Rick Wise, Program Director	Dr. Simon S. Ang, Thesis Director

Abstract

One of the objectives of this thesis work was to investigate the cathode performance of lithium cobalt oxide ($LiCoO_2$) incorporated with graphene powder in lithium ion batteries (LIBs). Graphene powder was incorporated into cathode materials to enhance the performance of LIBs. The other objective was to impede the construction of a solid electrolyte interphase (SEI) sheet using graphene sheet coating on its cathode.

The results of this work show that adding graphene powder improved the performance of $LiCoO_2$ as a cathode material. With the incorporation of different weight percentages of graphene powder, the LiBs showed distinct changes in their charging and discharging characteristics. The cell with its cathode incorporated with a 0.5 wt.% graphene powder exhibited the highest discharge capacity at currents 0.1 C and 0.5 C, The incorporation of 1 wt.% graphene powder contributed the most stable performance of the cathode at currents from 0.1 C to 2 C. In addition, the cell with its cathode incorporated with 2 wt.% graphene powder exhibited a higher discharge capacity of the cathode.

Conversely, the cathodes coated with one graphene sheet exhibited lower discharge capacity than that of the pristine cathode. This can be explained by the transfer limit of lithium ions as the graphene sheet blocked the electrolyte immersing into cathode materials, thus only part of cathode materials participate in the process of lithium ion transfer.

Acknowledgements

Firstly, I would like to offer my appreciation to Professor Simon S. Ang, my advisor of my master research, for his persistent guidance and encouragement throughout the last three years. He is an excellent teacher and a great inspiration to me.

Moreover, I would like to thank Dr. Huajun Andrew Zhao, my collaborator for this work, for his contribution and continued help during the process of research. Many of the experiments would not be finished without him. Moreover, I have learned many things from him, such as his passion and his experience with experiments.

I would like to thank Xingeng Yang, Xiumei Geng, and Xinsong Yang for their help to solve the problems I met.

I would like to thank everyone in the Microelectronics-Photonics Program. I will not forget the happy time working and living with them.

Furthermore, I am very thankful for my friends Hanlin Zhang, Qigen Yan, Siyuan Wang, Wenbo Xu, Chuaner Zhao, and others in Fayetteviile, Arkansas.

At last, I would like to thank my parents Yanjing Miao and Liwu Wang for their encouragement all the time. They are always supporting my decisions without any doubt. They are my inspiration and my best friends forever.

Table of Contents

List of Figures

List of Tables

Chapter 1: Introduction

The worldwide society development consumes countless energy, which is generally dependent on fossil fuels [1]. This is because the extraction and distribution of fossil fuels are generally relatively low cost [1]. However, many serious environmental issues are caused by fossil fuels combustion [2]. To find an alternative, energy storage systems are making use of the unique features of green energy sources, such as solar energy [3].

Battery storage is an effective technology for renewable energy [4]. Additionally, it is a common agreement that electrochemical batteries are the most reliable method [3]. Lithium ion batteries (LIBs) are one kind of electrochemical batteries. Since LIBs were introduced to market in 1991 by Sony [5], they have been widely applied in various fields.

The components of a LIB consists of two electrodes that includes a cathode and an anode, one or more separators made of polymer membrane, and the electrolyte. Lithium ion batteries have many advantages compared with other commercial secondary batteries. The advantages of LIBs are an extraordinary initial voltage, a long lifespan, and a high energy density [6]. However, there are also several weaknesses of both cathode and anode. Currently, anodes are facing one or more issues, such as low storage of Li, and irreversible capacity loss [7].

Graphene is a monolayer graphite with its carbon atoms [8]. Due to the honeycomb structure, several advantages of graphene including its high mechanical strength [7], good thermal conductivity, and great electronic mobility [9] have been explored. Its excellent electrical conductivity may increase storage capacity of lithium in LIBs [10] [11].

The SEI film is created by the reaction between active lithium metal and electrolyte [12]. For LIBs, the SEI layer determines the safety issue, and influences the irreversible capacity loss [13]. However, solid electrolyte interphase has a high resistance [14].

Therefore, the incorporation of graphene is a reasonable method to imrpove the performance of LIBs. Additionally, impeding the formation of SEI film is another expected way to increase the discharge capacity. These are the objectives of this thesis research.

Chapter 2: Introduction of Lithium Ion Batteries

2.1 Energy Storage Systems

Concerns such as environment pollution and global warming [2], lead to a strong encouragement to decrease the harmful effects from the process of generation and transportation of electric energy [15]. Energy storage systems (ESSs) are introduced to decrease the waste of energy to ensure a constant availability of renewable energy [15]. Energy systems can store and release energy by converting electrical energy to other forms of energy [15]. For energy storage systems, the reaction normally occurs between the electrodes and electrolyte [16].

Yoshino [17] reports the difference among batteries, fuel cells, and capacitors that are three main types of ESSs. A battery usually has one or more cells with many interactions to contribute electricity. Fuel cell, the device where electrochemical transformation occurs, offers one form of fuel and an oxidant. An electrochemical capacitor saves electrical energy in its electrical double layers whose formation is between the electrolyte and electronic conductor [16].

Winter and Brodd [16] present a more detailed comparison among these three forms of energy storage systems. They argue that the components of batteries, fuel cells and supercapacitors are similar which include one cathode, one anode, and an electrolyte. For batteries and fuel cells, the redox reactions are main sources to produce electrical energy. However, batteries and fuel cells have different locations to store and convert energy. Because they are a closed system, the process of storing and converting energy occurs at same place. On the other hand, however, fuel cells are open systems, thus their process of storing and converting energy occur at different compartments. In supercapacitors or electrochemical capacitors, “anode” and “cathode” are not proper, since energy is not generated through redox reactions.

Winter and Brodd [16] further reported the difference of application market among these three ESSs. Till now, batteries are considered as the most practical EES and have a dominating market evaluation, meanwhile the markets of supercapacitors are in memory protection for some electrical devices. However, fuel cells are in the process of developing and are still searching to find their best application for future market.

2.2 Lithium Ion Batteries (LIBs)

2.2.1 The Birth of LIBs

Throughout the 1980s, the development of rechargeable batteries was being pushed by the energy requirements of portable electronic devices [17]. However, widely used rechargeable batteries, such as lead-acid batteries and nickel-metal hydride (NiMH) batteries, had severe size or weight disadvantages [17]. Therefore, a new form of batteries was needed at that time.

Primary (disposable) batteries and secondary (rechargeable) batteries are different forms of batteries [16]. A primary battery consists of one or several connected cells, can provide electrical energy, and is discarded after its stored energy is exhausted. In contrast, a secondary battery has the ability to be recharged to its original charged capacity after its stored energy is exhausted.

Winter and Brodd [16] pointed out the initial state difference between disposable batteries and rechargeable batteries. The initial state of primary batteries is fully charged, and discharging is the major reaction when the batteries are working. However, rechargeable batteries have normally been discharged and then need to be charged to store electrical energy before discharge in a secondary process.

In the early 1980s, Akira Yoshino [17] had the idea of LIBs and then made a practical LIB battery in 1986. A LIB can be described as “a nonaqueous secondary battery using

transition-metal oxides containing lithium ion such as $LiCoO_2$ as a positive electrode and carbonaceous materials as a negative electrode [17]."

Goodenough et al. [17] firstly pointed out the usage of $LiCoO_2$ as a cathode in 1979. In 1982, Yazami and Touzain [18] successfully demonstrated the electrochemical intercalation in LIBs along with graphite as the anode material. Graphite is still a common anode materials in LIBs nowadays.

In 1986, Akira Yoshino [17] successfully achieved the first safety tests on LIBs. In 1991, after further development, Sony introduced the first LIBs to commercial markets [5]. Akira Yoshino [17] listed several advantages of LIBs as follows:

1) It has a larger energy density compared with NiCd batteries or NiMH batteries at same physical conditions.
2) It has a good reduction in the size and weight that fits in portable devices.
3) It can supply electrical energy for a cell phone with only one cell due to a 4 volts or more voltage.

Notebook computers and cell phones drive the demand of the portable device market [9]. Fig. 2.1 indicates the market of LIBs.

Lithium ion batteries market expands rapidly and are expected to keep increasing [17]. In addition, as a commonly used energy storage device, lithium ion batteries have more challenges caused by electric vehicles (EVs) and hybrid electric vehicles (HEVs), which have been two revolutionary technologies nowadays [19]. On the other hand, the huge and promising market of LIBs have also pushed the development in several fields, such as material research areas (carbonaceous materials, polymers, and ceramics), and the related areas, such as electrochemistry, electrical packaging, chemical materials, physical materials and surface chemistry [17].

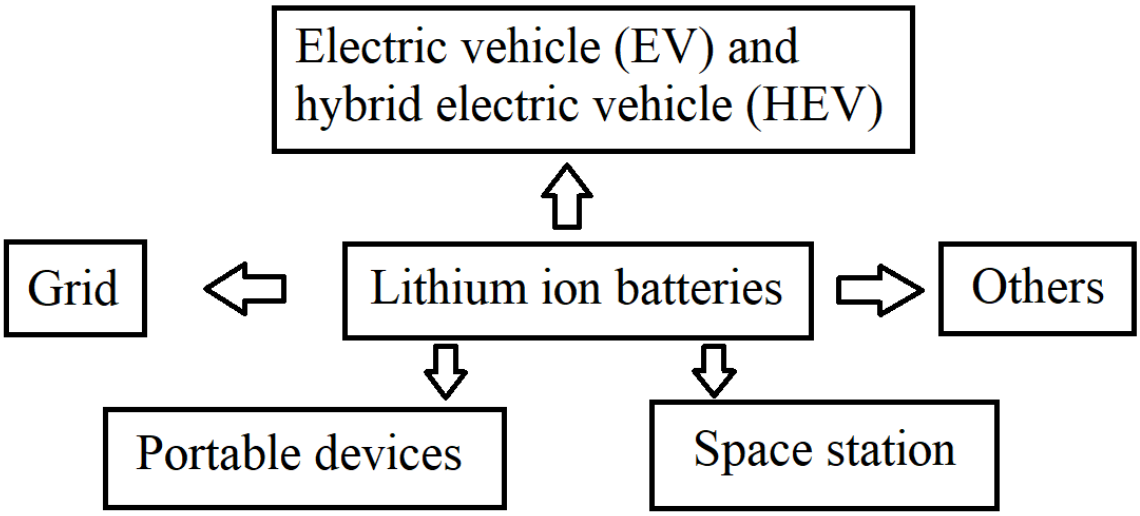

Fig. 2.1. The market of LIBs.

2.2.2 Operation of LIBs

A LIB battery are made of an anode, a cathode, the electrolyte, and one or more separators as shown in Fig. 2.2.

Yoshino [17] introduced roles of each material in a LIB. The anode, as the negative electrode, is the location of the oxidation reaction and releases electrons. The positive electrode of a cell, cathode, is where reduction reactions occur, and receives electrons coming from the anode. The electrolyte contributes to the conductivity between the cathodes and anodes.

The most popular electrolyte used in the LIBs is lithium hexafluorophosphate ($LiPF_6$) salt mixed with solvent mixtures such as ethylene carbonate (EC). Dimethyl carbonate (DMC), diethyl carbonate (DEC), and ethyl methyl carbonate (EMC) are common linear carbonates [20].

The separator is an obstacle between the cathode and anode used for inhibiting a short-circuit from occurring in a cell. Separators have several forms, such as a polymer with extremely small holes and inactive materials immersed in electrolyte. Note that they are designed to allow

ions to go through as well as be passive all the time.

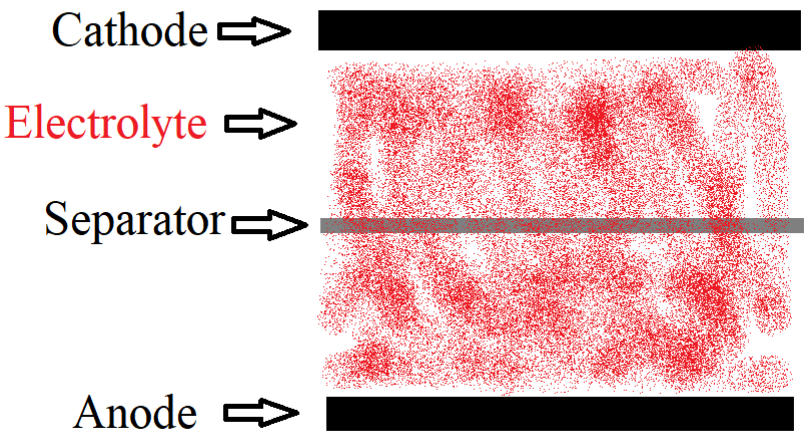

Fig. 2.2. The components of a LIB.

Fig. 2.3 shows the process of charge and discharge in the lithium ion batteries. Lithium ions can drive through the cathode and anode. Typically, both the cathode and anode in a LIB consist of intercalation compounds and they allow Li^+ to be inserted into their structures [7]. When the battery is being charged, Li^+ extracts from cathode and intercalates into anode. Conversely, Li^+ swim from anode to cathode when battery is being discharged.

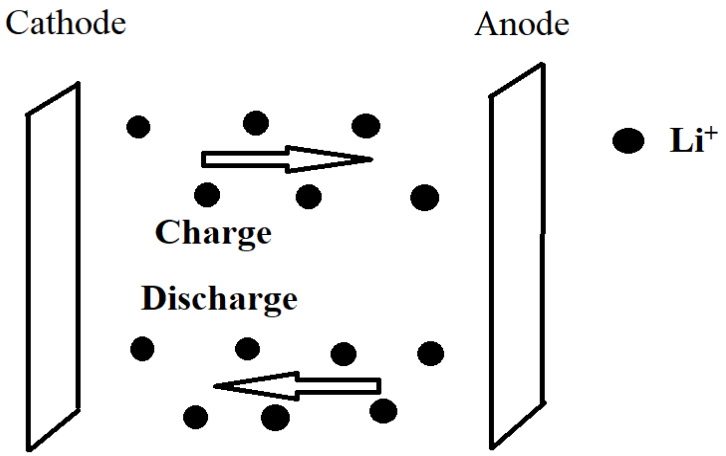

Fig. 2.3. The operation of LIBs.

The positive electrode half-reaction during the process of charging is [21]:

$$LiCoO_2 \leftrightarrow Li_{1-x}CoO_2 + xLi^+ + xe^- \quad \text{(Equation 2.1)}$$

The negative electrode half-reaction at the same time is [21]:

$$xLi^+ + xe^- + 6C \leftrightarrow LixC_6 \quad \text{(Equation 2.2)}$$

where C is carbon.

The combined overall reaction is:

$$LiCoO_2 + C \leftrightarrow Li_{1-x}CoO_2 + CLi_x \quad \text{(Equation 2.3)}$$

When x is 0.5, the theoretical capacity is 372 mAh/g [21].

Any overcharge or over-discharge would be harmful to the LIBs. Mahmood and Hou [21] indicated that overcharging and over-discharging or supersaturating the cathode would destroy the cell due to irreversible reactions as shown below [21]:

$$LiCoO_2 \rightarrow Li^+ + CoO_2 + e^- \quad \text{(Equation 2.4)}$$

$$LiCoO_2 + e^- + Li^+ \rightarrow Li_2O + CoO \quad \text{(Equation 2.5)}$$

2.2.3 Characteristics

Currently, $LiCoO_2$ is a common cathode for commercial LIBs since it has a high capacity and a great cyclability [22]. The major considerations for LIBs consist of energy density, power

density, and others [5]. As such, over-delithiation causes an around 9% volume contraction [22].

Several advantages and disadvantages are listed below [16], [23]:

Advantages:

1. A higher energy density (twice higher than NiCd batteries).
2. A high cell voltage (3.6 V).
3. Work in harsh envrionment.
4. It can operate in any orientation.
5. Different sizes and shapes.
6. Long lifetime.

Disadvantages:

1. A relative low energy capacity (10^{-3} S/cm).
2. Several safety issues.

2.3 Related Research Based on LIBs

Many researches are investigated to strengthen the performance of LIBs in several aspects, such as cathode, anode, and electrolyte [3], [20], [24-30].

2.3.1 Research on Electrolytes

The most popular electrolyte for LIBs is $LiPF_6$ salt dissolved in EC, DMC, DEC, and EMC [20]. This is based on the several characteristics of such electrolyte. Lithium hexafluorophosphate ($LiPF_6$) has the capability to passivate, and thus, protects aluminum (Al), Ethylene carbonate (EC) can provide a high ionic conductivity [20]. Ethyl methyl carbonate (EMC) has proven to have the best thermal compatibility with EC [24].

Zhang et al. [20] used $LiPF_6$- EC-EMC as the electrolyte for a cell whose electrodes were spinel $LiMn_2O_4$ and graphite to determine a supreme ratio of $LiPF_6$/EC-EMC for LIBs. As a result, Zhang et al. [20] demonstrated an ideal ratio of electrolyte for LIBs is 1M $LiPF_6$ 3:7 EC-EMC.

Much attention is currently being focused on the investigation of why some electrolytes have better stability and reality than the liquid organic carbonate solutions do [3]. Ionic liquid solution (ILs) is one of liquid organic solutions. One disadvantage of ILs is that its organic ions could suffer unexpected structure change [25]. Scrosati et al. [3] also indicated there is still a long path for ionic liquid solutions to find their applications as an electrolyte for LIBs.

2.3.2 Research on Anodes

The electrical conductivity of one layer walled CNTs is 10^6 S/m at 300 K and the conductivity of multi-layer CNTs is over 10^5 S/m for the same condition. Single-walled carbon nanotubes have reversible capacities ranging from 300 to 600 mAh/g, which are larger than those of graphite [29-32]. However, it is not easy to produce CNTs with a desired size or structure [26].

Graphitic carbon is an anode material for many commercial LIBs. However, metals can be used as an alternative due to their higher capacities compared with graphite [26]. During the process of forming alloys, metals have the capability to store more Li^+ than graphite can [26]. For example, one Al atom or one Sn atom can compound with two to four Li^+, whereas graphite needs to provide six carbon atoms to insert one lithium ion [27], [28]. This advantage offers metal-based anodes a larger storage capacity when volume expansion occurs [28]. When the battery is in discharging state, Li^+ are driven to the positive electrode and the metal alloys return to their original state by shrinking back to its initial size [26].

2.3.3 Research on Cathodes

The most common materials used as cathode materials for LIBs contain $LiCoO_2$, $LiFePO_4$, and $LiMnO_4$ [5]. $LiFePO_4$ and $LiMnO_4$ have been investigated for many years [5], [19]. Lithium iron phosphate ($LiFePO_4$) has a good theoretical capacity and a stable cyclability [33]. However, its conductivity for electrons and Li^+ is low [5]. Lithium manganate ($LiMnO_4$) is expected to be used as electric vehicle (EV) batteries since it requires a low cost [34] and offer a safer environment [35]. One of its weaknesses is its relatively low cyclability [5].

Lithium sulfur (Li-S) and lithium air (Li-air) batteries can provide extraordinary energy densities thanks to the reaction of Li^+ with sulfur (S) and O_2 to form Li_2S and Li_2O_2, separately [21]. Mahmood and Hou [21] reported the delivery of pure oxygen is a major issue for Li-air batteries since air consists of different gases which are harmful for cells and can decrease its capacity. A lithium sulfur battery has its own limits, such as polysulfide anions transport.

Chapter 3: Carbonaceous Materials of LIBs

3.1 Overview of Carbonaceous Materials

Over the past several decades there has been great development in nanotechnology, which is fundamentally applied for the materials with sizes below 100 nm [36]. Fullerenes are well-known nanoscale materials that are made of carbon and exist in different forms, such as sphere, ellipsoid, and tube [36].

Carbon exists in the forms of diamond, graphite, and fullerenes [37]. Graphite has a layer structure and its carbon atoms arrange in its hexagonal structure within one layer. Fig. 3.1 shows that graphite layers are stacked in the AB sequence [37].

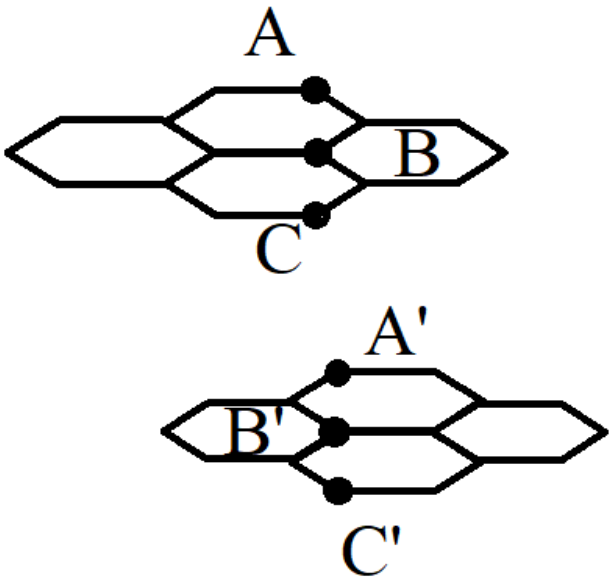

Fig. 3.1. The structure of graphite layers.

The first individual graphene planes were successfully isolated by Novoselov et al. in 2004 [38], while the graphite structure has long been known. References 39 and 40 suggest that graphene has huge potential to be used for electrical energy storage devices.

3.2 Graphene

3.2.1 General Characteristics

Graphene is one layer graphite and its carbon atoms arrangement forms a honeycomb structure [8] as shown in Fig. 3.2. Each carbon atom is a surface atom due to its honeycomb structure, which indicates that each graphene atom is a surface atom [6]. Graphene has the highest intrinsic mechanical strength, a large surface area [7], and good electronic mobility [9].

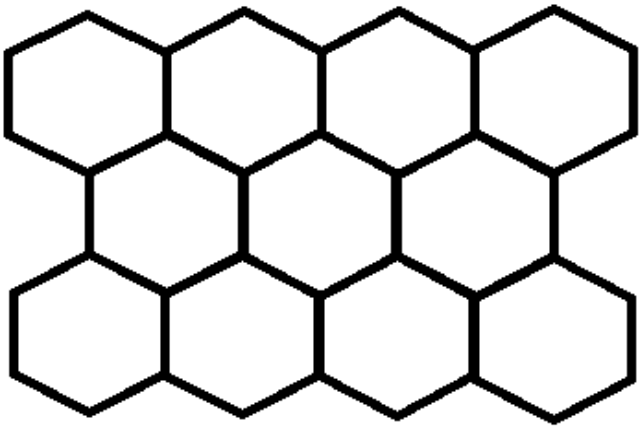

Fig. 3.2. The arrangement of graphene atoms.

Graphene is monolayer graphite [36-40]. Geim and Novoselov [8] questioned what are the least number of layers of graphene when it can be regarded as a 3D structure. Different layer structures reflect distinct properties of graphene due to the weak bonds among layers [8], [41].

3.2.2 Graphene Preparation

The synthesis of graphene on a large scale has been achieved [42]. Several techniques such as mechanical exfoliation of oriented graphite [6], coating on the surface of SiC [43], conversion from graphene oxide (rGO) [44], as well as chemical vapor deposition (CVD) [45]

are common methods to gain graphene. The methods used for its preparation depend on the size and the properties of graphene layers required. Mechanical exfoliation [6] and precipitation on a silicon surface [43] cannot be used for large scale production. Wide-ranging graphene layers fabrication is possibly reached by CVD method or chemically converting from rGO [42]. The graphene sheets prepared from the CVD method have less resistance than those prepared from the solution-phase graphene oxide method. Therefore, CVD is commonly used when high quality graphene is desired [42].

3.3 Related Research

3.3.1 General Overview

Currently, investigations of new energy sources are encouraged by increasing demand of electrical devices [46]. Lithium ion batteries (LIBs) have several advantages compared with other conventional batteries [6]. Lithium intercalation compounds are common cathode materials for LIBs [5], [6]. However, there are some disadvantages of these materials which limit their applications, such as limited lithium ions storage and large capacity loss [7]. For example, carbon and tin-based materials can both provide good cyclability with low original efficiency and high irreversible capacity loss, respectively [47].

Due to its electrical conductivity of 10^{-4} S/cm, graphene has potential to be an extraordinarily proper component in LIB cathodes [5]. In addition, graphene may also improve storage capacity of Li^+ for lithium ion batteries [10], [11]. Goosey [36] introduced the different performance of graphene when added into cathode materials. When cathode materials consisting of graphene are mixed properly, a conducting network is formed for electrons in LIBs. However, when mixed in disproportionate amounts of graphene, it can impede the transfer of lithium ions.

Studies [33] show that graphene, limited by its low coulombic efficiency and weak stability, cannot be considered as a cathode or an anode.

Nevertheless, graphene could be considered as an excellent material when used as an additive to increase the conductivity for cathodes [36].

3.3.2 Graphene Used in Anode Materials

The anode is playing an essential role in LIBs. Currently, graphite is a frequently used anode. Its low theoretical capacity can be one limitation that restricts its application in EVs and HEVs [19]. Therefore, other materials have to be examined to replace graphite.

Non-carbon-based anodes are being researched. Nowadays, tin-based electrode, silicon-based electrode, and transition metal based electrode are three major investigated anode materials for LIBs. For the case of these three anode materials, the incorporation of graphene can provide a good electrical conductivity and a high surface area [6]. Moreover, graphene is chemically and thermally stable which help to keep electrodes working in harsh environments [6].

3.3.2-1 Tin-Based Materials

Tin (Sn) and its oxides, such as SnO_2, are popularly investigated for the anode materials [6], [19]. SnO_2 has a higher theoretical capacity compared with graphite [19]. However, serious volume variation occurs when lithiation or delithiation in process [6]. The reaction is shown below [6]:

$$Sn + 4.4Li + +4.4e^- \leftrightarrow Li_{4.4}Sn \qquad \text{(Equation 3.1)}$$

This reaction destroys the electrical connection with the anode [3]. Liang et al. [48] indicated that the interpretation of tin-based anodes was enhanced due to the incorporation of graphene.

3.3.2-2 Silicon-Based Materials

Silicon and lithium ions can form $Li_{4.4}Si$ when silicon is used as an anode material [6]. The reaction is [49]:

$$Si + 4.4Li + +4.4e^{-} \leftrightarrow Li_{4.4}Si \qquad \text{(Equation 3.2)}$$

It has a large charge capacity and a low discharge voltage [6]. The volume of Si increases up to 270% due to the formation of $Li_{3.75}Si$ during the process of discharge [6]. This weakens the stability of transfer [50]. The incorporation of graphene can increase the transport capability for both electron and lithium ions [6].

3.3.2-3 Transition Metal-Based Materials

Transition metal oxides are probable anodes since lithium storage capacity of these materials is over 600 mAh/g [6], [19]. The reaction is [19]:

$$nano\text{–}MO + 2Li \leftrightarrow nano\text{–}M + Li_2O \qquad \text{(Equation 3.3)}$$

where M = Fe, Co, or Cu.

The volume of those materials increases during lithiation process due to the formation of Li_2O [19]. For another example, Co_3O_4 has an 890 mAh/g theoretical capacity and its volume expands during the processes of charging and discharging [6]. Adding graphene decreases

volume expansion as well as restrains the detachment and collection of metal oxide [19].

Manganese oxide (Mn_3O_4) has a great theoretical capacity with a low electrical conductivity, which limits its actual maximum capacity [6]. Zhu et al. [6] demonstrated that the incorporation of graphene can provide the cathode Mn_3O_4 a great ratio capacity of delithiation ~900 mAh/g.

3.3.3 Graphene Used in Cathode Materials

3.3.3-1 $LiMn_2O_4$

Lithium manganese oxide ($LiMn_2O_4$) as the cathode materials has many advantages including high electronic conductivity [19], environmental friendliness, and high abundance of manganese (Mn) [51]. However, its low theoretical capacity (148 mAh/g) changes during the cycling [19]. In addition, Mn^{2+} dissolves into the electrolyte, which lowers the reversible capacity [52].

Bak et al. [35] reported that the incorporation of graphene sheets helps to increase the conductivity of bare $LiMn_2O_4$ cathode. It has been shown that $LiMn_2O_4$/graphene sheet composites have a good reversible capacity [6]. Zhao et al. [53] synthesized $LiMn_2O_4$/graphene composite enhanced both the stability of cycling and theoretical capacity.

$LiMn_2O_4$ doped with other molecules ($LiM_xMN_{2-x}O_4$, M = Ni, Fe, Co, etc.) has been recommended to restrict Mn^+ dissolving in the electrolyte [19]. Prabakar et al. [54] reported that electrons can transfer faster after adding graphene into cathode materials to form a sandwiched $LiNi_{0.5}Mn_{1.5}O_4$-graphene composite as a cathode.

3.3.3-2 $LiFePO_4$

$LiFePO_4$ is a potential cathode since its theoretical discharge capacity is larger than that

of $LiCoO_2$ and it has a low toxicity [19]. On the other hand, its capacity fades quickly under a high rate of charge or discharge due to its low electrical conductivity and a weak transport ability [6], [55]. Its electrical conductivity of 10^{-14} S/cm is lower than those of $LiCoO_2$ and $LiMn_2O_4$, which are 10^{-9} S/cm and 10^{-6} S/cm, respectively [19].

The incorporation of graphene could increase the conductivity of electrode [6]. In addition, graphene could strength the cycling stability due to its mechanical properties [6]. There are several methods, such as hydrothermal, solvothermal, and solid state routes, to prepare $LiFePO_4$/graphene composite [6], [55].

Su et al. [56] used graphene to replace one fourth weight percentage of carbon additive. The results showed that the charging transfer resistance decreased due to the increased electrical conductivity.

Ding et al. [57] indicated that the initial capacity of $LiFePO_4$ incorporated with graphene is 160 mAh/g at 0.2 C compared with bare $LiFePO_4$ cathode whose capacity is 113 mAh/g [19], [57].

Several papers [56], [58], [59] show that adding graphene could decrease the capacity fade. The capacity decreases 3% at 30^{th} cycle at 0.1 C [56], 300^{th} cycle at 5 C [58], and 5% at 1000^{th} cycle at 20 C [59]. These results demonstrate that $LiFePO_4$/graphene composite retain the stability of the cathode during the process of charge and discharge. There is no further research to prove the exact mechanism for the great cyclability of $LiFePO_4$/graphene composite [5]. However, papers [60] and [61] showed that strengthening the electronic connection among particles can enhance the cyclability of $LiFePO_4$/graphene composite.

3.3.3-3 $Li_3V_2(PO_4)_3$

The voltage range of this material is 3.0 – 4.3 V during the process of intercalation and

extraction [62]. The theoretical capacity of $Li_3V_2(PO_4)_3$ is 197 mAh/g [63], but it has a low electronic conductivity such as 240 nS/m at 25 ^oC [6].

The incorporation of graphene increases its electrochemical performance [38]. Huang et al. [62] and Yu et al. [63] used sol-gel, solid-state, and spray-drying method to prepare $Li_3V_2(PO_4)_3$ /graphene composite.

Lu et al. [19] and Liu et al. [64] indicate that $Li_3V_2(PO_4)_3$/graphene cathode has an increased rate capability and an enhanced stability during cycling due to the formation an electrical conducting network consisting of graphene. The cost is a potential issue for the application of graphene in the cathode materials, since incorporating with even a low weight ratio will cost more [19].

The advantages of composites of materials incorporated with graphene can be summarized as follows [6]. The incorporation of graphene impedes the volume expansion of metal electrodes when they are being charged and discharged. Moreover, the life cycle of LIBs has capability to be enhanced. Graphene increases the conductivity of metal electrode materials. Adding graphene can increase the rate performance of cathodes and anodes by controlling the growth of metal oxide particles. The combination of graphene increases the lithium storage capacity of metal oxide materials.

3.4 Summary and motivation

LIBs play an essential part in several areas, such as portable devices including notebook computers, cell phones, EVs and HEVs.

The performance of LIBs mainly relies on their anodes and cathodes. However, many disadvantages of the cathode and anode limit its usage. For example, the anode has a limited Li storage capacity, a low capability of charge and discharge rate, and poor capacity retention. For

the case of the cathode, the low electrical conductivity of common cathode materials needs to be enhanced to satisfy the desires for batteries with higher performance.

Graphene, as a single layer graphite with a honeycomb structure, has been considered as a suitable additive to LIBs since it was discovered in 2004. From above discussions, the performance of electrodes is enhanced by the incorporation of graphene. Moreover, adding graphene improves the physical and chemical properties in some aspects. However, there is little research on incorporating graphene into $LiCoO_2$ as a cathode of LIBs which is the subject of this research work.

SEI film exists between electrodes and electrolyte. The formation of this layer is due to the reaction between the electrolyte and active lithium metal. However, the SEI film has a high resistance. To investigate the performance of LIBs without this high resistance, the formation of SEI layer should be avoided.

In this work, two methods were prepared to incorporate graphene into $LiCoO_2$ electrodes. One was adding different weight percentages of graphene powder into cathodes to augment the performance of $LiCoO_2$ as the cathode. The other one was coating a graphene sheet (6 – 8 layers) on the pristine electrode to impede the formation of SEI layer.

Chapter 4: Experiment

4.1 Overview of Materials

The materials used in this research were lithium cobalt oxide ($LiCoO_2$) (Fig. 4.1(a)), super P carbon black (Fig. 4.1(b)), N- Methyl-2-pyrrolidone (NMP) (Fig. 4.1(c)), poly(vinylidene fluoride) (PVDF) (Fig. 4.1(d)), electrolyte, separator, and graphene including graphene powder and graphene sheet (6-8 layers).

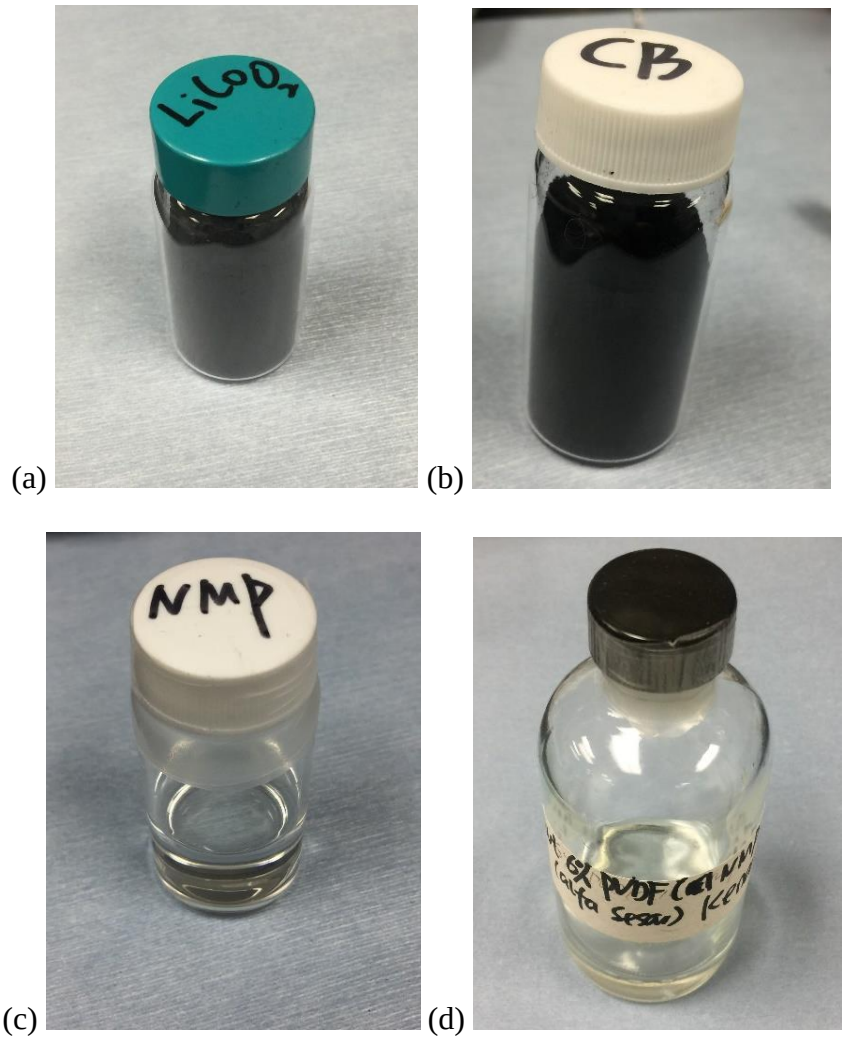

Fig. 4.1. Materials of cathode: a) lithium cobalt oxide ($LiCoO_2$), b) super P carbon black, c) N-Methyl-2-pyrrolidone (NMP), and d) poly(vinylidene fluoride) (PVDF).

PVDF powder was purchased from Sigma-Aldrich Co [65]. $LiCoO_2$, carbon black, and NMP were purchased from Alfa Aesar Co [66]. Graphene nanopowder was purchased from Graphene Supermarket Co [67]. Graphene sheet (6-8 layers) was purchased from ACS Materials Co [68].

4.2 Roles of Materials

4.2.1 $LiCoO_2$

$LiCoO_2$ is one major cathode material for LIBs in this research since it has a capacity of 272 mAh/g [22] with an energy density of around 3.5 g/cc [23].

4.2.2 Carbon Black

Super P carbon black has a surface zone of 62 m^2/g [69] and is used as an electronic conductor to improve the conductivity of $LiCoO_2$, which was the cathode in this research. Dominko and his co-workers [70] reported that carbon black was essentially needed to determine the performance of the cathode. It must be noted that carbon black or other electrical conductors have to be evenly mixed in the cathode materials [71].

The working mechanism of carbon black is shown in the Fig. 4.2. In order to avoid severe polarization, both lithium ions and electrons have to be inserted at the same place as shown in Fig 4.2(b) [71]. However, a low reversible capacity occurs if there is any part of active particles not contacting with electronic conductor carbon black particles (Fig 4.2(a)) because electrons would be reflected in the polarization [71]. For the case of $LiCoO_2$, a low content of evenly dispersed carbon black can give cathodes a better performance than a high content of unevenly mixed carbon black [71].

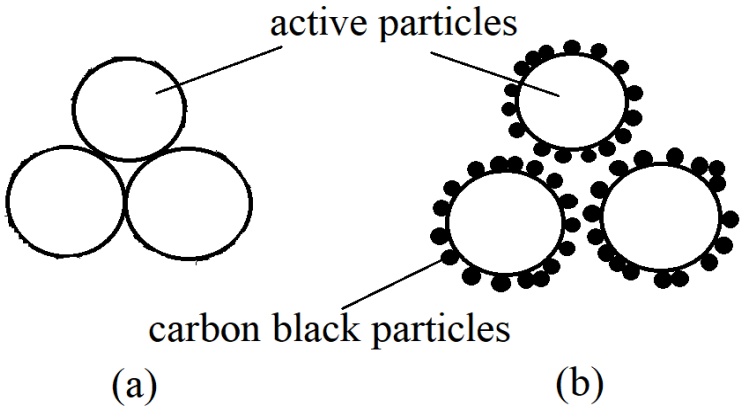

Fig. 4.2. The mechanism of electrode a) without carbon black and b) with carbon black.

There are other applications of carbon black in batteries [72-74]. For example, carbon black is commonly used as cathode for Li-O_2 batteries [72]. In addition, carbon black, as an anode active additive, has been used for LIBs [73]. Kim et al. [74] demonstrated that a high density of LIBs is achieved by directly coating carbon black on the cathodes.

4.2.3 NMP

NMP is commonly used to dissolve carbon-based compounds [75]. In this research, NMP was used for dispersing oxide material, which enhances capacitive utilization of oxide [76]. Moreover, a stable suspension could be achieved by NMP, an organic solvent, and poly(vinylidene fluoride) [77], which was the binder for cathode materials. Noting that NMP is toxic, the operations related to NMP had to be performed inside a fume hood for this research.

4.2.4 PVDF

Poly(vinylidene difluoride) (PVDF) is a binder to preserve the electrode, or the

electrode would be crumbled [78]. PVDF is a common binder for commercial LIBs due to its outstanding electrochemical stability and bonding strength [78].

4.2.5 Separator

The separator is used to inhibit the contact between the cathode and anode [77]. Normally, nonwoven fabrics and microporous polymeric films are two main types of separators [79]. A less than 25 μm fabric with desired requirements is hard to be produced; microporous polymeric films are most widely used as a separator in commercial LIBs [77]. In this research, microporous polymeric films were used to separate the cathode and anode. A good separator should have the following properties: low ionic resistance [80], high chemical stability against electrolyte, and high mechanical stability [77]. In contrast, however, thicker separators can offer better mechanical strength during assembly, thus improving the safety of LIBs [81]. The pore size of a separator should be particularly minute to impede the permeation of particles, or it could cause a short circuit [77], [81].

There are several copolymers of PVDF, such as poly(vinylidene fluoride-hexafluoropropylene) (PVDF-HFP) [82] and poly(vinylidene fluoride-co-chlorotrifluoroethylene) (PVDF-CTFE) [83] used as separators in the LIBs. There are many advantages of PVDF and its copolymers. For example, d_{33} value of poly(vinylidene fluoride-tetrafluoroethylene (PVDF-TFE) is -38 pC/N [84].

4.2.6 Electrolyte

In this research, 1M $LiPF_6$ 3:7 EC–EMC was used as the electrolyte in LIBs as recommended [20]. There are several advantages [20]: $LiPF_6$ can passivate and protect the Al, which is controlling the current; and EC-EMC has a high dielectric content to give rise to a high

ionic conductivity.

4.3 Cathode Preparation

4.3.1 Pristine Cathode and Cathode with Graphene Sheet

The weight percentage of each material was 80% $LiCoO_2$, 10% super P carbon black, and 10% PVDF as recommended from references 82 and 85. The PVDF powder was dissolved in NMP to yield 6% by weight PVDF in NMP. It was reported that 6% could be the maximum concentration for the PVDF solution in NMP [85]. All materials were poured into a plastic tube. Extra NMP – double volume of PVDF liquid – was added into the same tube. Extra NMP was added to decrease the viscosity of composite which could be uniformly poured on the aluminum (Al) foil. Nitrogen was introduced into the plastic tube to remove the ambient oxygen. This was because oxygen would influence the mixture of electrode components. A VWR (model VM-3000) [86] as shown in Fig. 4.3(a) was used to mix the composite inside the plastic tube for at least 90 minutes. A maxmium speed of 3500 revolutions per minute (rpm) was used. Above 3500 rpm, the composite slurry would accumulate at the top of the tube and make the composite not uniform. This was followed by ultrasonic vibration of the composite at a frequency of 20 kHz for two hours in a Branson 3500 ultrasonicator [87] as shown in the Fig. 4.3 (b).

4.3.2 Cathode with Graphene Powder

The graphene powder was first ultrasonically vibrated in the NMP for two hours. Different weight percentages (0.5 wt.%, 1 wt.%, and 2 wt.%) of graphene powder were transferred through droppers into three separate tubes. The weight of the graphene was calculated according to the percentage of molecular weights of carbon black, $LiCoO_2$, and PVDF. Next, they were ultrasonicated for two hours in the Branson 3500 ultrasonicator.

(a) 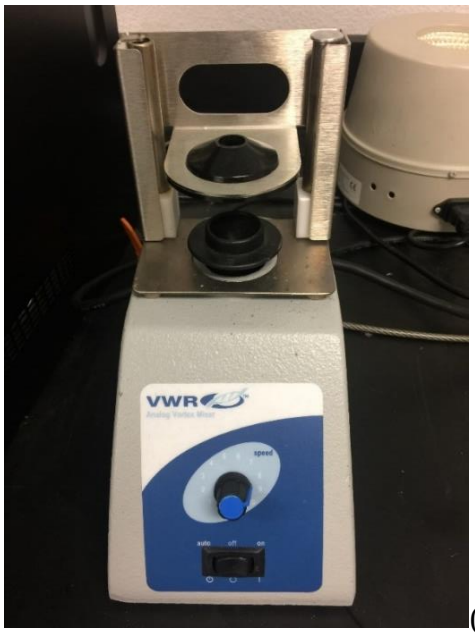

(b) 

Fig. 4.3. a) VWR mixer, b) Branson 3500 ultrasonicator.

4.4 Electrode Fabrication

4.4.1 Pristine Cathode and Electrode with Graphene Composite

The electrode was prepared on the Al foil with the slurry of $LiCoO_2$, graphene powder, carbon black, and 6% PVDF dissolved in the NMP after ultrasonication. Samples were dried at room temperature under vacuum overnight. Then samples were pressed at about 20 MPa by a PHI manual compression press [88].

4.4.2 Cathode Coated with Graphene Sheet

To obtain unbroken graphene sheet, copper (Cu) foil beneath the graphene sheet was etched away using a 0.7 mol/L iron nitrate ($Fe(NO_3)_3$) solution in deionized water (DI water) [24]. Tweezers were used to lightly place the Cu foil with graphene sheet on the surface of solution. After etching for 20 minutes, the transparent graphene sheet floated to the top of

solution. A dropper was used to remove the $Fe(NO_3)_3$ solution and DI water was injected slowly to prevent destroying the graphene sheet. After several careful DI water rinses and making sure there was no impurity in the water, the pristine electrode was gently slid into water, and moved beneath the graphene sheet. The remaining water was then removed using a dropper and the sample was dried overnight. The electrodes were ready after being fully dried.

4.5 Button Cell Assembly

4.5.1 Glove Box Instruction

Button cells were assembled in the MBraun glove box [89] as shown in Fig. 4.4.

Fig. 4.4. Mbraun glove box.

To correctly operate the glove box, these steps should be followed. To move materials into the glove box, materials should be placed into the inlet tube on the right side of the glove box with a vacuum indicator as shown in Fig. 4.5 (a). The inlet door is first locked. The concentration of O_2 and H_2O should be adjusted to less than 1 part per million (ppm) using the

touch screen. The handle, as shown in Fig. 4.5(b), is switched to the left to exhaust the air in the inlet cylinder; the pressure in the inlet cylinder will become lower. Three minutes is required to achieve -25 in Hg vacuum. Cylinder should be refilled with nitrogen after three minutes until the pressure is -15 inHg inside the cylinder. The evacuating and refilling steps are repeated three times. Note that, for the third time, refilling the cylinder ends when the pressure is 0 in Hg instead of -15 in Hg.

(a) 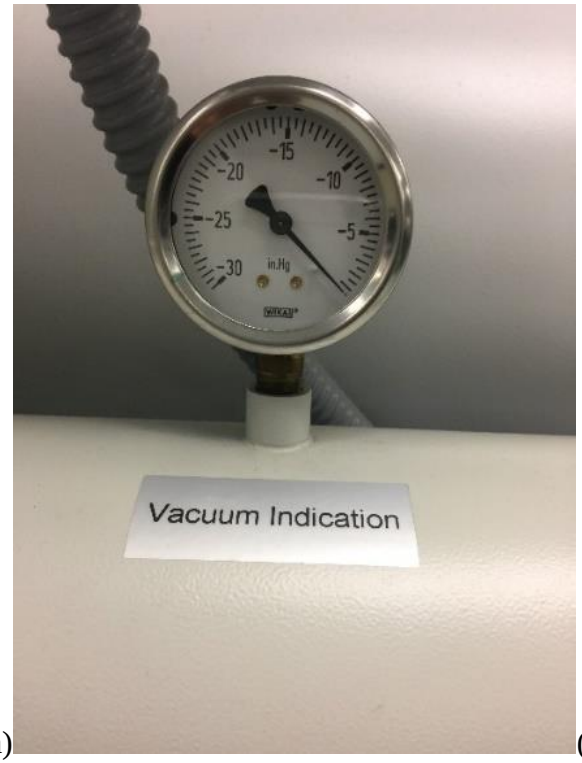

(b) 

Fig. 4.5. The glove box: a) pressure indicator, and b) handle for pump-purging.

To bring materials out from the inlet cylinder, it must first be evacuated. Materials are placed in the glove box through the inside door connected to inlet cylinder. This inside door should be securely locked before the materials are picked up or the oxygen would fill the glove box and pollute the environment inside.

4.5.2 Assembly Process

To ensure the electrodes were completely dried without any water, all samples were placed into the glove box for 12 hours before assembly. The concentrations of oxygen and water inside glove box were under 2 parts per million. Celgard 3501 microporous membranes [90] were used as separators in the button cells.

Fig. 4.6 shows the structure inside of an assembled button cell. From top to bottom, “a” is a wave washer, “b” is a lithium chip, “c” is a lithium foil, “d” consist of two separators, and “e” is the cathode. All samples are assembled in order from bottom to top. One thing to note is that all these components should not touch the button cell wall or it would cause a short circuit for the button cell.

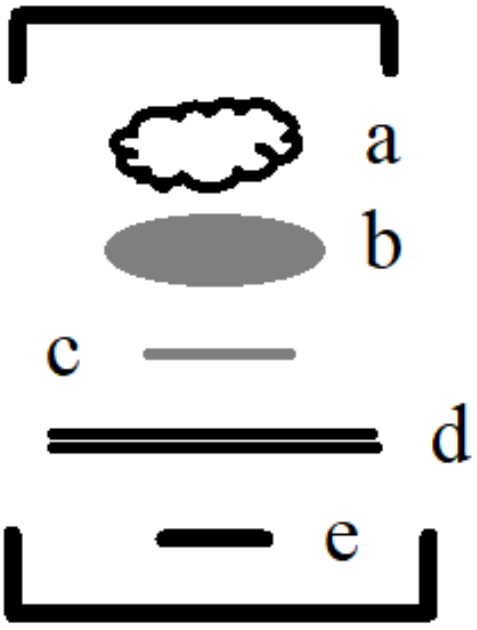

Fig. 4.6. The structure of the CR2032 button cell.

Fig. 4.7 shows two sides of button cells after being assembled. The negative side (Fig. 4.7(a)) has a dotted textured surface while the positive terminal (Fig. 4.7(b)) has a number on the

surface. CR2032 type button cells have a lip that pulls over from the positive side to encase the negative side.

(a)

(b)

Fig. 4.7. CR2032 button cells: a) negative electrode side, and b) positive electrode side.

4.6 Button Cell Tests

4.6.1 Testing equipment

A CHI660D electrochemical analyzer [91] was used to express the electrochemical impedance spectroscopy (EIS) measurements of cathode samples. The frequency range was 1 Hz - 1 MHz and the amplitude was 5 mV. A BT2000 battery tester [92] was used for full cycles of charging and discharging. To test the performance under different rates of charging and discharging, four current conditions were set. The four current conditions, 0.1 C, 0.5 C, 1 C, and 2 C, represent the rate of charging or discharging from slow to fast. A current of 0.1 C represents the current that can fully charge or discharge the capacity of a cell in ten hours.

4.6.2 Data Presentation of Battery Tester

Fig. 4.8 shows a continuous and integrated process of charging and discharging for 5 cycles under a similar condition. The blue plot presents the current while the pink plot is the voltage. When the value of current was positive, the button cell was being charged as its cell voltage was increased. A process of charging and discharging represents one cycle. There was no obvious change of current and voltage during five cycles, thus, this sample was still a stable integrated button cell after the fifth cycle.

Table 4.1 shows the data collected from the battery tester. These parameters consist of the number of cycles, test time, date, current, voltage, and maximum voltage on each cycle. In addition, some other parameters, such as capacities and energies, are also shown in Table 4.1.

The test current can be calculated as:

$$I_t = (M_{cathode} - M_{Al\ foil}) * 80\% * 140\ mAh \qquad \text{(Equation 4.1)}$$

Table 4.1. Test data of the button cell.

Cycle Index	Test Time(s)	Date Time	Current(A)	Voltage (V)	Charge Capacity (Ah)	Discharge Capacity(Ah)	Charge Energy(Wh)	Discharge Energy(Wh)	Charge Time(s)	Discharge Time(s)	Vmax On Cycle(V)
1	59222	3/12/2017 7:22	-2.35E-05	3	0.00021	0.000179	0.000837	0.00071	31852	27364	4.3
2	118061	3/12/2017 23:43	-2.36E-05	3	0.0002	0.00018	0.000823	0.000714	31360	27474	4.3
3	176609	3/13/2017 15:59	-2.35E-05	3	0.0002	0.00018	0.000812	0.000717	30965	27579	4.3
4	235099	3/14/2017 8:13	-2.36E-05	3	0.0002	0.000182	0.000805	0.000722	30725	27759	4.3
5	293418	3/15/2017 0:25	-2.35E-05	3	0.0002	0.000182	0.0008	0.000723	30515	27799	4.3

where I_t is the testing current, $M_{cathode}$ is the weight of cathode sample, $M_{Al\ foil}$ is the weight of Al foil, 80% is the weight percentage of $LiCoO_2$ in the cathode materials, and 140 mAh/h is the reversible capacity of $LiCoO_2$.

The unit for charge/discharge capacity is ampere-hour (Ah) shown in the Table. 4.1, which indicates the capacity during each cycle. In addition, the capacity depends on the mass of cathode. However, each cathode sample cannot have an exactly same mass. The unit of charge and discharge capacity is "mAh/g" in this research. Therefore, the discharge capacity would be independent of the different weight of each cathode sample.

Ampere-hour can be converted to mAh/g using

$$C_{dis}\,(mAh/g) = Cdis\ (Ah) / [(M_{cathode} - M_{Al\ foil}) * 80\%] \qquad \text{(Equation 4.2)}$$

where C_{dis} (mAh/g) is the value of converted discharge capacity, C_{dis} (Ah) is the value of discharge capacity obtained from battery tester, $M_{cathode}$ is the weight of cathode sample, $M_{Al\ foil}$ is the weight of Al foil, and 80% is the weight percentage of $LiCoO_2$ in the cathode materials.

Table 4.1 and Fig. 4.8 represent the data of one cell of cathode sample 01081-2. The weight of this cathode was 4.95 mg and the weight of Al foil was 2.5 mg. Therefore, using Eq. 4.1, the test current value was ~2.35×10^{-5}A, which was the value of current for 1 C. 1 C stands for the current that can fully discharge a battery in one hour. The discharge capacity (mAh/g) of this sample at the first cycle was ~104.64 mAh/g using Eq. 4.2.

4.6.3 Electrochemical Impedance Spectroscopy

In this research, a CHI 660D [91] was used to exhibit the EIS measurements and to study the complex electrochemical resistance in the assembled button cells. The initial voltage was 3.2 V and the range of frequency was 1 MHz - 1 Hz, as well as the amplitude was 0.005 V.

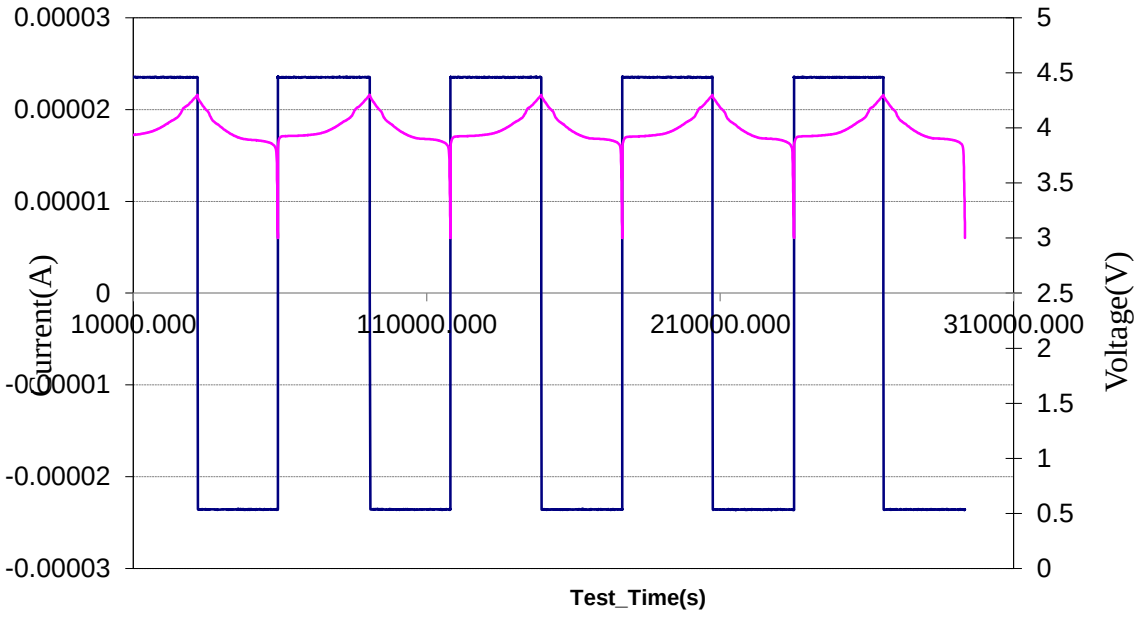

Fig. 4.8. The plot of current (A) (pink), voltage (V) (blue) vs test times (s) obtained from the battery tester.

4.6.3-1 Impedance and Resistance

Impedance is a complex resistance [93] and is used to describe the capability to resist electrical current. Electrical resistance obeys Ohm's law:

$$R = \frac{\mathrm{E}}{\mathrm{I}} \qquad \text{(Equation 4.3)}$$

where E is the voltage, and I is the current.

In practical world, circuit elements exhibit complex properties. Therefore, impedance is introduced to replace resistance. Moreover, impedance is not limited by Ohm's law mentioned above.

4.6.3-2 Impedance Data Presentation

EIS is a common measurement for detecting the impedance of a system [94]. Moreover, EIS data are commonly represented in Nyquist plots [93]. Fig. 4.10 shows a Nyquist plot. The expression of impedance consists of two parts: a real resistance and an imaginary impedance. The real resistance is shown on the X axis and the imaginary impedance is shown on the Y axis as shown in Fig. 4.9 [95]. Imaginary impedance consists of the capacitive and inductive reactance [96]. Note that the value of imaginary impedance is always negative [95]. The left part of a Nyquist plot represents higher frequencies while the right side represents the lower frequencies [97]. The vector with a length |Z| represents for the impedance, and phase angle is the angle between vector and real resistance axis [94]. The impedance at one frequency is one point shown in the Nyquist plot, but the value of frequency is not shown [95]. The charge transfer resistance is represented as the diameter of half circle shown in the Fig. 4.9 [93]. It was needed to analyze charge transfer resistance collected from Nyquist plots through EIS measurements in this work.

4.6.3-3 Advantages

There are several advantages of EIS as follows [94], [96]:

1. Several parameters can be indicated simultaneously through an EIS measurement.
2. EIS can be used when a more precise measurement is required.
3. EIS is extremely helpful to investigate the corrosion protection by organic coatings.

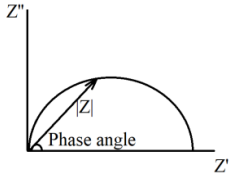

Fig. 4.9. The Nyquist plot.

Chapter 5: Results and Discussion

Several samples for each type were successfully tested, however, only one sample for each condition is presented and discussed in this chapter.

5.1 Sample with Pristine Cathode

Fig. 5.1 shows the charge and discharge capacity of a typical sample with pristine cathode under four current situations (0.1 C, 0.5 C, 1 C, and 2 C).

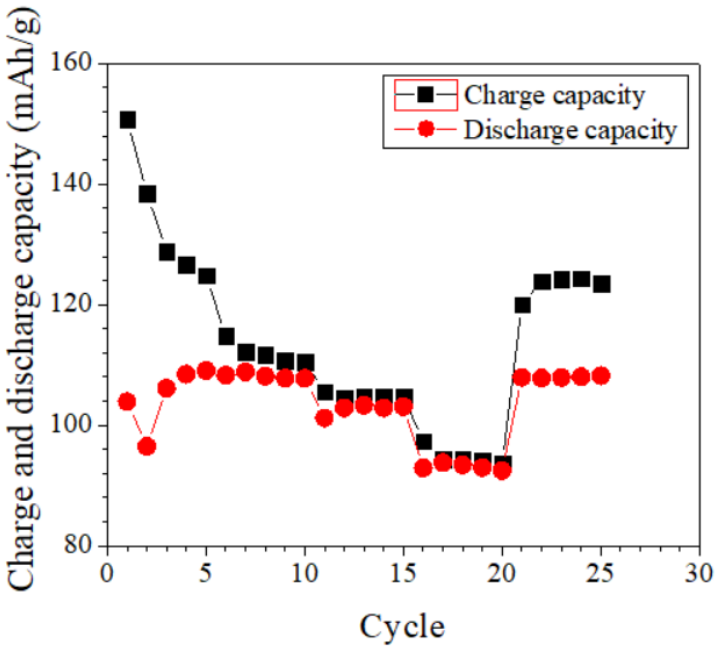

Fig. 5.1. The charge and discharge capacities of a typical pristine cathode sample.

In this plot, each point was the value of capacity at only one cycle. The average values of charge capacity under same current were 129.77 mAh/g, 111.99 mAh/g, 104.84 mAh/g, 94.76 mAh/g, respectively. Discharge capacities of the sample were stable under each current situation. The average values of discharge capacity under 0.1 C, 0.5 C, 1 C, 2 C were 86.96 mAh/g, 83.02

mAh/g, 65.99 mAh/g, and 31.26 mAh/g, respectively. These values are shown in Table 5.1. In addition, discharge capacity decreased when the current was increased.

Table 5.1. Test data of a pristine cathode from battery tester.

Cycle	Current (A)	Charge Capacity (mAh/g)	Discharge Capacity (mAh/g)	Vmax On Cycle (V)	Current (C)
1	-2.248E-05	150.71	78.92	4.30V	0.1
2	-2.248E-05	138.51	87.92	4.30V	0.1
3	-2.248E-05	128.86	89.4	4.30V	0.1
4	-2.248E-05	126.65	89.42	4.30V	0.1
5	-2.248E-05	124.83	89.19	4.30V	0.1
6	-0.0001128	114.8	83.36	4.30V	0.5
7	-0.0001128	112.2	83.27	4.30V	0.5
8	-0.0001127	111.65	82.94	4.30V	0.5
9	-0.0001128	110.74	83.03	4.30V	0.5
10	-0.0001129	110.56	82.52	4.30V	0.5
11	-0.0002242	105.56	63.45	4.30V	1
12	-0.0002245	104.4	65.13	4.30V	1
13	-0.0002243	104.84	65.21	4.30V	1
14	-0.0002246	104.69	65.55	4.30V	1
15	-0.0002246	104.73	65.63	4.30V	1
16	-0.000449	97.32	29.91	4.30V	2
17	-0.000449	94.39	30.76	4.30V	2
18	-0.000449	94.47	31.43	4.30V	2
19	-0.000449	94.08	32.02	4.30V	2
20	-0.000449	93.57	32.18	4.30V	2
21	-2.248E-05	119.99	87.26	4.30V	0.1
22	-2.248E-05	123.91	87.71	4.30V	0.1
23	-2.248E-05	124.3	87.43	4.30V	0.1
24	-2.248E-05	124.37	86.66	4.30V	0.1
25	-2.248E-05	123.5	86.45	4.30V	0.1

EIS measurements were used to monitor the sample every five cycles. Fig. 5.2 is the Nyquist plot of the typical cell with a pristine cathode. The curves at middle height in the plot represent the charge transfer resistance [81]. The Nyquist plot shows that the charge transfer resistance was stable ranging from -40 to -80 Ω at the imaginary part (Z'' axis). Fig 5.2 shows that all curves tend to infinity, which indicates an increasing resistance for lithium ions transfer. This can be explained by the breakdown of electrolyte and the increased thickness of SEI film [12].

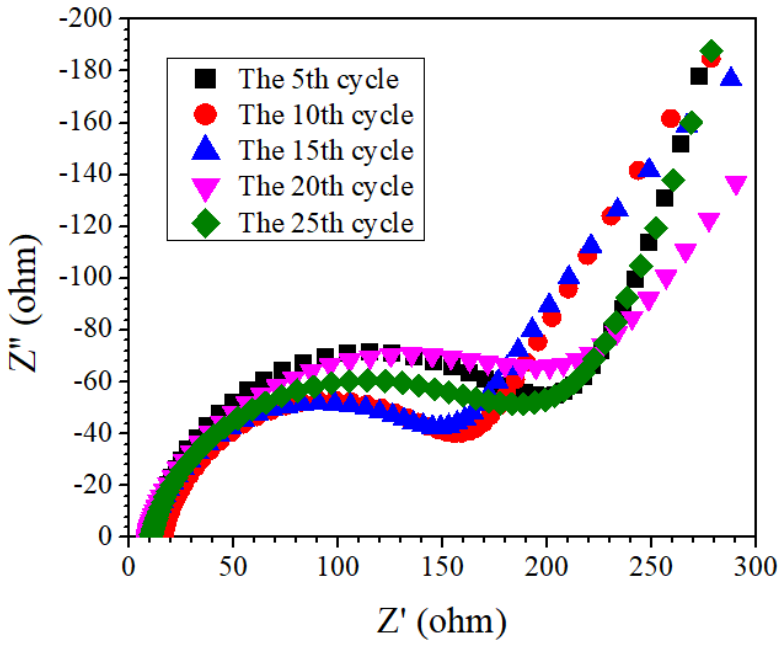

Fig. 5.2. Nyquist plot of a pristine cathode sample.

5.2 Sample Incorporated with Graphene Powder

5.2.1 0.5 wt.% Graphene Powder

The charge and discharge capacity values of the cell with a cathode incorporated with 0.5 wt% graphene powder are shown in Fig. 5.3. The average values of charge capacity under four

current situations were 166.34 mAh/g, 153.93 mAh/g, 135.81 mAh/g, 120.31 mAh/g, respectively. From Table 5.2, the average values of discharge capacity under same current conditions were 112.74 mAh/g, 111.97 mAh/g, 102.01 mAh/g, and 90.41 mAh/g, respectively.

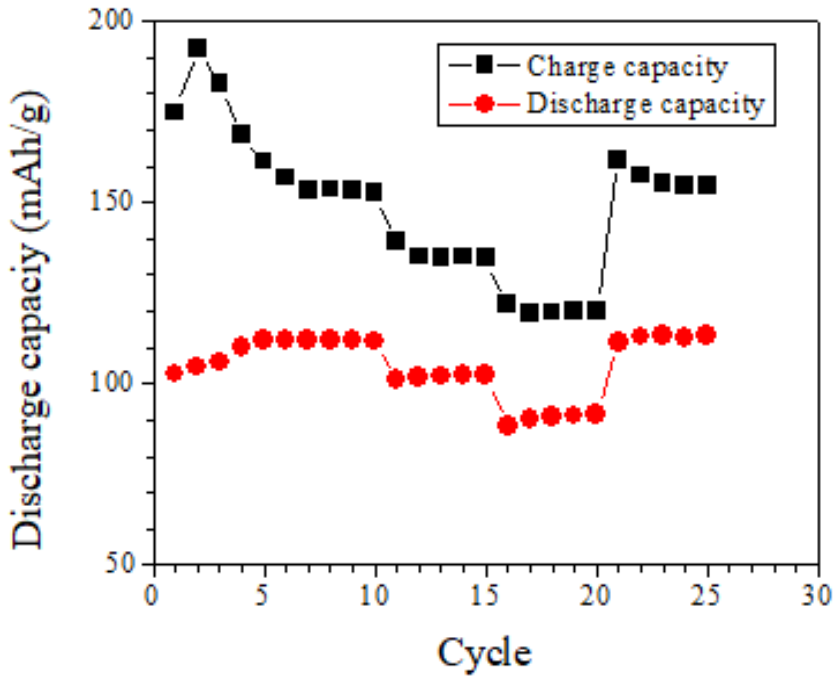

Fig. 5.3. Charge and discharge capacity of a typical cathode incorporated with 0.5 wt.% graphene powder.

From the Nyquist plot shown in Fig. 5.4, charge transfer resistance became stable after the initial cycle. Electrolyte might not fully fill the entire button cell when the cathode sample was first assembled. Therefore, it was reasonable to show an odd initial curve which represents a high charge transfer resistance.

Compared to the Nyquist plot of the pristine sample (Fig. 5.2), the charge transfer resistance did not change much after the incorporation of 0.5 wt.% graphene powder. Moreover, at different current conditions, the discharge capacity increased for the cell after adding 0.5 wt.% graphene powder into its cathode materials.

Table 5.2. Test data of a cathode with 0.5 wt.% graphene powder from battery tester.

Cycle	Current (A)	Charge Capacity (mAh/g)	Discharge Capacity (mAh/g)	Vmax On Cycle (V)	Current (C)
1	-2.86E-05	174.79	102.67	4.30V	0.1
2	-2.86E-05	192.57	104.72	4.30V	0.1
3	-2.86E-05	182.75	105.92	4.30V	0.1
4	-2.85E-05	168.66	110.05	4.30V	0.1
5	-2.86E-05	161.24	111.85	4.30V	0.1
6	-0.000143	156.72	112.16	4.30V	0.5
7	-0.000143	153.39	112	4.30V	0.5
8	-0.000143	153.67	112.03	4.30V	0.5
9	-0.000143	153.21	111.88	4.30V	0.5
10	-0.000143	152.64	111.77	4.30V	0.5
11	-0.000285	139.05	101.29	4.30V	1
12	-0.000285	135.13	101.99	4.30V	1
13	-0.000285	134.89	102.19	4.30V	1
14	-0.000285	135.04	102.33	4.30V	1
15	-0.000285	134.94	102.27	4.30V	1
16	-0.000571	122.06	88.54	4.30V	2
17	-0.000571	119.63	90.37	4.30V	2
18	-0.000571	119.72	90.59	4.30V	2
19	-0.000571	119.99	91.26	4.30V	2
20	-0.000571	120.17	91.52	4.30V	2
21	-2.85E-05	161.71	111.53	4.30V	0.1
22	-2.85E-05	157.57	112.99	4.30V	0.1
23	-2.86E-05	155.17	113.19	4.30V	0.1
24	-2.86E-05	154.45	112.57	4.30V	0.1
25	-2.85E-05	154.49	113.42	4.30V	0.1

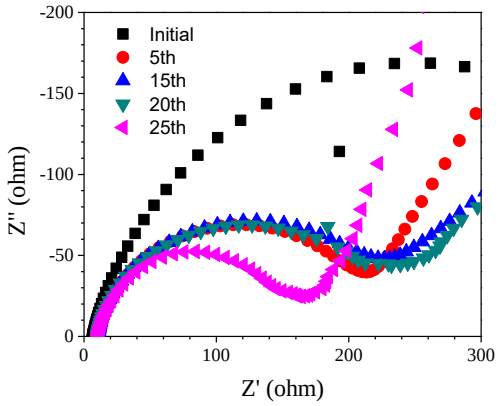

Fig. 5.4. Nyquist plot of a typical cathode incorporated with 0.5 wt.% graphene powder.

5.2.2 1 wt.% Graphene Powder

Fig. 5.5 reports the charge and discharge capacity values of a typical cathode incorporated with 1 wt.% graphene powder. For this sample, the average values of charge capacity under same currents were 116.91 mAh/g, 107.53 mAh/g, 72.64 mAh/g, 39.66 mAh/g, respectively. In addition, the average values of discharge capacity under different current conditions were 107.53 mAh/g, 109.23 mAh/g, 105.73 mAh/g, and 99.52 mAh/g, respectively, as given in Table 5.3.

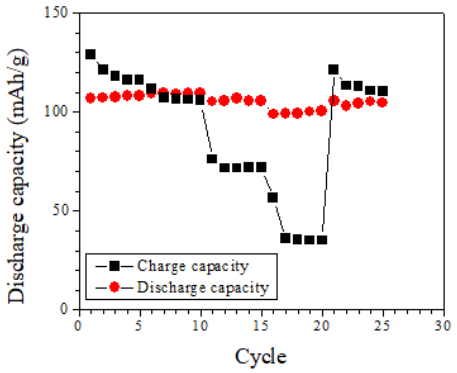

Fig. 5.5. Charge and discharge capacity of a typical cathode incorporated with 1 wt.% graphene powder.

Table 5.3. Test data of a cathode with 1 wt.% graphene powder from battery tester.

Cycle	Current (A)	Charge Capacity (mAhg)	Discharge Capacity (mAhg)	Vmax On Cycle (V)	Current (C)
1	-2.63E-05	128.91	106.63	4.30V	0.1
2	-2.63E-05	121.18	107.04	4.30V	0.1
3	-2.63E-05	118.13	107.45	4.30V	0.1
4	-2.63E-05	116.35	108.2	4.30V	0.1
5	-2.64E-05	116.19	108.34	4.30V	0.1
6	-0.000131	111.72	109.18	4.30V	0.5
7	-0.000131	107.38	109.28	4.30V	0.5
8	-0.000131	106.57	109.11	4.30V	0.5
9	-0.000131	106.28	109.32	4.30V	0.5
10	-0.000131	105.69	109.26	4.30V	0.5
11	-0.000263	76.09	105.25	4.30V	1
12	-0.000263	71.58	105.4	4.30V	1
13	-0.000263	71.69	106.78	4.30V	1
14	-0.000263	71.96	105.61	4.30V	1
15	-0.000263	71.87	105.6	4.30V	1
16	-0.000526	56.58	98.8	4.30V	2
17	-0.000526	36.05	99.13	4.30V	2
18	-0.000526	35.52	99.17	4.30V	2
19	-0.000526	35.06	100.21	4.30V	2
20	-0.000526	35.08	100.27	4.30V	2
21	-2.629E-05	121.25	105.49	4.30V	0.1
22	-2.625E-05	113.19	103	4.30V	0.1
23	-2.625E-05	112.98	104.26	4.30V	0.1
24	-2.625E-05	110.77	105.28	4.30V	0.1
25	-2.632E-05	110.17	104.69	4.30V	0.1

From the Nyquist plot shown in Fig. 5.6, the charge transfer resistance tends to become stable after the fifth cycle. Compared with the Nyquist plot of the cell with a pristine cathode (Fig. 5.2), the charge transfer resistance increased with the addition of 1 wt.% graphene powder. In addition, the discharge capacity of a cathode incorporated with 1 wt.% graphene powder was higher than that of the cell with a pristine cathode under different current conditions.

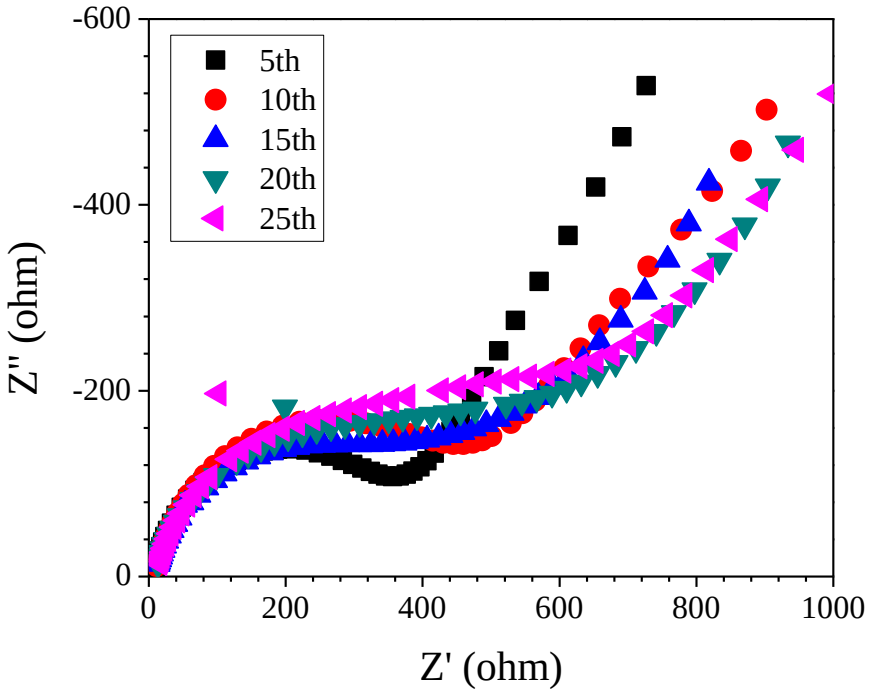

Fig. 5.6. Nyquist plot of a cathode incorporated with 1 wt.% graphene powder.

5.2.3 2 wt% Graphene Powder

Figure 5.7. shows the average values of charge and discharge capacity of a typical cell with its cathode incorporated with 2 wt.% of graphene powder under 0.1 C, 0.5 C, 1 C, and 2 C. The average values of charge capacity were 122.19 mAh/g, 104.13 mAh/g, 78.45mAh/g, 50.61 mAh/g, respectively. The average values of discharge capacity were 98.11 mAh/g, 93.58 mAh/g, 75.87 mAh/g, and 48.13 mAh/g, respectively, as shown in Table 5.4.

Table 5.4. Test data of a cathode with 2 wt.% graphene powder from battery tester.

Cycle	Current (A)	Discharge Capacity (mAh/g)	Discharge Capacity (mAh/g)	Vmax On Cycle (V)	Current (C)
1	-1.905E-05	136.83	101.34	4.50	0.1
2	-1.905E-05	136.09	98.33	4.50	0.1
3	-1.905E-05	134.36	98.48	4.50	0.1
4	-1.905E-05	140.91	97	4.50	0.1
5	-1.905E-05	155.39	95.39	4.50	0.1
6	-9.552E-05	111.62	95.73	4.50	0.5
7	-9.552E-05	107.07	94.6	4.50	0.5
8	-9.553E-05	103.22	92.94	4.50	0.5
9	-9.552E-05	100.51	92.94	4.50	0.5
10	-9.552E-05	98.22	91.69	4.50	0.5
11	-0.0001905	85.33	76.08	4.50	1
12	-0.0001905	71.22	77.51	4.50	1
13	-0.0001905	80.32	75.65	4.50	1
14	-0.0001905	78.46	75.64	4.50	1
15	-0.0001904	76.91	74.46	4.50	1
16	-0.000381	55.25	48.81	4.50	2
17	-0.000381	51.17	48.99	4.50	2
18	-0.000381	49.85	48.32	4.50	2
19	-0.000381	48.82	47.64	4.50	2
20	-0.000381	47.97	46.89	4.50	2
21	-1.905E-05	93.94	95.9	4.50	0.1
22	-1.905E-05	110.12	97.17	4.50	0.1
23	-1.905E-05	106.74	95.59	4.50	0.1
24	-1.905E-05	105.46	94.44	4.50	0.1
25	-1.905E-05	102.03	92.95	4.50	0.1

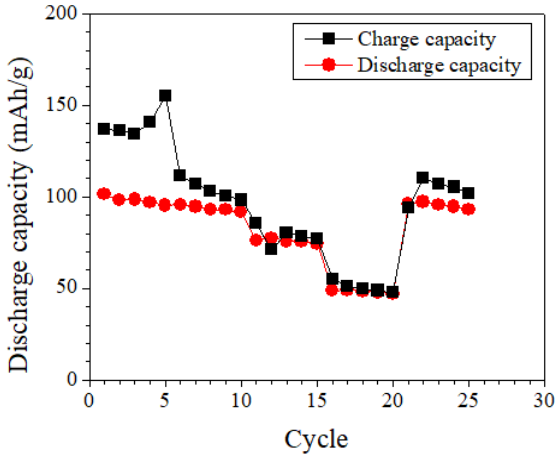

Fig. 5.7. Charge and discharge capacity of a cathode incorporated with 2 wt.% graphene powder.

Fig. 5.8 shows a very high charge transfer resistance at the initial cycle. Each sample was tested immediately after it had been assembled. However, after five cycles of charge and discharge, the Nyquist plot (Fig. 5.9) indicates that a cell with its cathode incorporated with 2 wt.% graphene powder had an extremely low charge transfer resistance. The charge transfer resistance obviously decreased after the incorporation of 2 wt.% graphene powder. The discharge capacity increased about 20 mAh/g after adding 2 wt.% graphene powder.

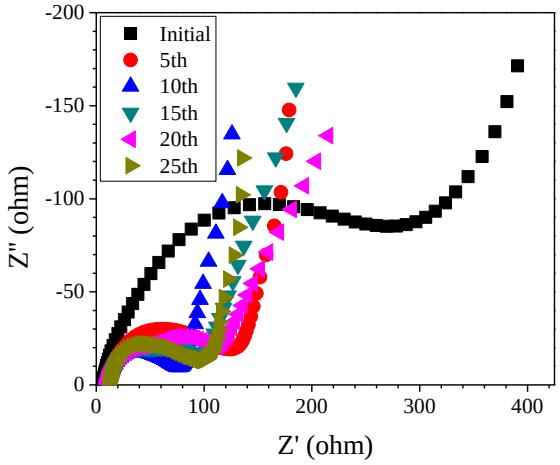

Fig. 5.8. Nyquist plot of a cathode incorporated with 2 wt.% graphene powder.

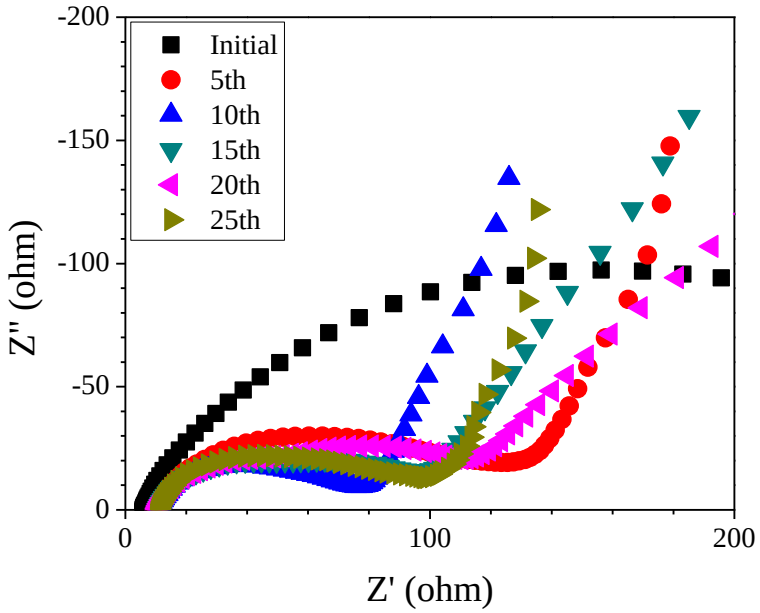

Fig. 5.9. Zoom in on Z' = 0-200 ohm for the Nyquist plot of cathode incorporated with 2 wt.% graphene powder.

Fig. 5.10 shows that incorporation of graphene powder into cathode materials increases the discharge capacity under different current conditions. The discharge capacity of a pristine cathode was really low, which means the performance of the cathode was not good under high current conditions. However, with the incorporation of 0.5 wt.% and 1 wt% graphene powder into the cathode, the discharge capacity significantly improved at high current (2 C). Adding 2 wt.% graphene powder enhanced the discharge capacity at 2 C current, even if the improvement was not as much as for samples with 0.5 wt.% and 1 wt.% graphene powder. When samples were tested at low current (0.1 C and 0.5 C), 0.5 wt% graphene powder had the most active capability to enhance the performance of cathodes. Samples with 1 wt.% graphene powder had the most stable performance ranging from 99 mAh/g to 110 mAh/g at different current conditions. At the mid-current, 1 C, discharge capacity of the cathode could be enhanced by adding 1 wt.% graphene powder.

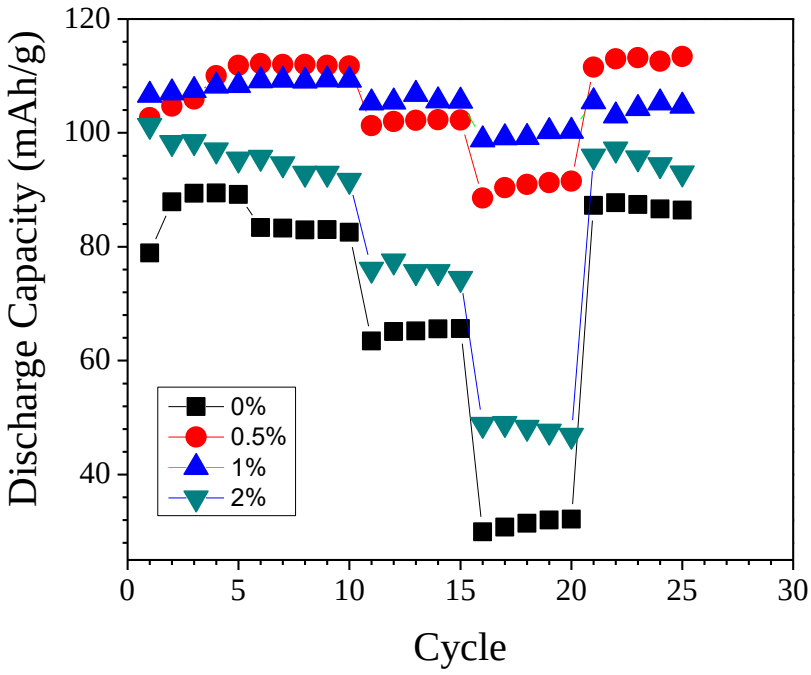

Fig. 5.10. Comparison of discharge capacity among pristine cathode and cathodes with graphene powder.

At low current, Fig. 5.10 indicates that the discharge capacity decreased when the weight percentage of graphene powder was increased. However, there was no such result shown at mid-current, 1C. Therefore, further work could focus on the influence of weight percentage of graphene powder to cathode performance. In contrast, the charge transfer resistance significantly decreased due to the incorporation of 2 wt.% graphene powder.

Graphene has very high electrical conductivity as mentioned in the Chapter 2 and 3. A very small amount of graphene can boost the conductivity of the electrodes. However, excessive graphene can increase the self-discharge and, thus, lower the discharge capacity. Reference 36 reported that when mixed at an improper ratio, graphene can impede Li^+ transfer. In addition, reference 33 pointed out that graphene is not a suitable electrode in LIBs.

Tang et al. [98] incorporated graphene nanosheets into $LiCoO_2$ and reported that 1 wt.%

is enough to build a network, which can significantly enhance the performance of the cathode. However, similar cycling performance was obtained for the conditions 1 wt.% and 2 wt.%. In this research, the performance of cathodes incorporated with 1 wt.% and 2 wt.% graphene powder were extremely different. Since 2 wt.% had shown less discharge capacities, there should be one peak value between 1 wt.% to 2 wt.%.

5.3 Sample Coated with Graphene Sheet

Fig. 5.11 shows that an increase of charge transfer resistance occurs after coating graphene sheet on the cathode. The odd initial curve could be explained by the unstable electrochemical system. However, the charge transfer resistance was still too high after the fifth cycle. When the cathode assembly became stable, it obtained a higher charge transfer resistance compared to the pristine cathode as well as other samples incorporated with graphene powder.

The average values of discharge capacity of the sample under different currents shown in Fig. 5.12 are 62.55 mAh/g, 62.37 mAh/g, 56.18 mAh/g, and 46.47 mAh/g, respectively, as shown in Table 5.5. In addition, the average values of charge capacity were 73.11 mAh/g, 65.68 mAh/g, 57.36 mAh/g, 45.53 mAh/g, respectively. Compared with the discharge capacity value of a pristine cathode (Fig. 5.1), the discharge capacity of cathode coated with graphene sheet decreases at different current situations as shown in Fig. 5.13. The results of high charge transfer resistance and lower discharge capacity can be explained by the working mechanism of a cathode coated with graphene sheet. Since coating graphene sheet on cathode can impede the formation of SEI layer, the structure inside the button cell changes.

Wang et al. [99] indicated that graphene sheet impedes Li^+ transfer. Fig. 5.14 shows the working mechanism of cathodes. Without graphene sheet coating, the cathode could release and accept Li^+ through the electrolyte (Fig. 5.14 (a)).

Table 5.5. Test data of a cathode coated with graphene sheet from battery tester.

Cycle	Current (A)	Discharge Capacity (mAh/g)	Discharge Capacity (mAh/g)	Vmax On Cycle (V)	Current (C)
1	-9.537E-06	99.64	60.53	4.30V	0.1
2	-9.573E-06	76.91	62.73	4.30V	0.1
3	-9.537E-06	72.67	63.25	4.30V	0.1
4	-9.573E-06	71.36	63	4.30V	0.1
5	-9.537E-06	70.21	63.26	4.30V	0.1
6	-4.758 E-05	66.33	62.19	4.30V	0.5
7	-4.758E-05	65.58	62.53	4.30V	0.5
8	-4.758E-05	65.11	62.45	4.30V	0.5
9	-4.758 E-05	65.81	62.47	4.30V	0.5
10	-4.758 E-05	65.58	62.33	4.30V	0.5
11	-9.515E-05	58.28	55.44	4.30V	1
12	-9.518E-05	57.26	56.13	4.30V	1
13	-9.511E-05	57.38	56.48	4.30V	1
14	-9.515E-05	56.55	56.55	4.30V	1
15	-9.518E-05	57.31	56.29	4.30V	1
16	-0.000190	49.08	45.03	4.30V	2
17	-0.000190	47.41	46.3	4.30V	2
18	-0.000190	47.76	46.94	4.30V	2
19	-0.000190	47.78	47.1	4.30V	2
20	-0.000190	35.61	47	4.30V	2
21	-9.537E-06	68.48	61.58	4.30V	0.1
22	-9.573E-06	68.13	61.52	4.30V	0.1
23	-9.573E-06	67.34	61.53	4.30V	0.1
24	-9.644E-06	68.36	61.44	4.30V	0.1
25	-9.644E-06	68.1	61.25	4.30V	0.1

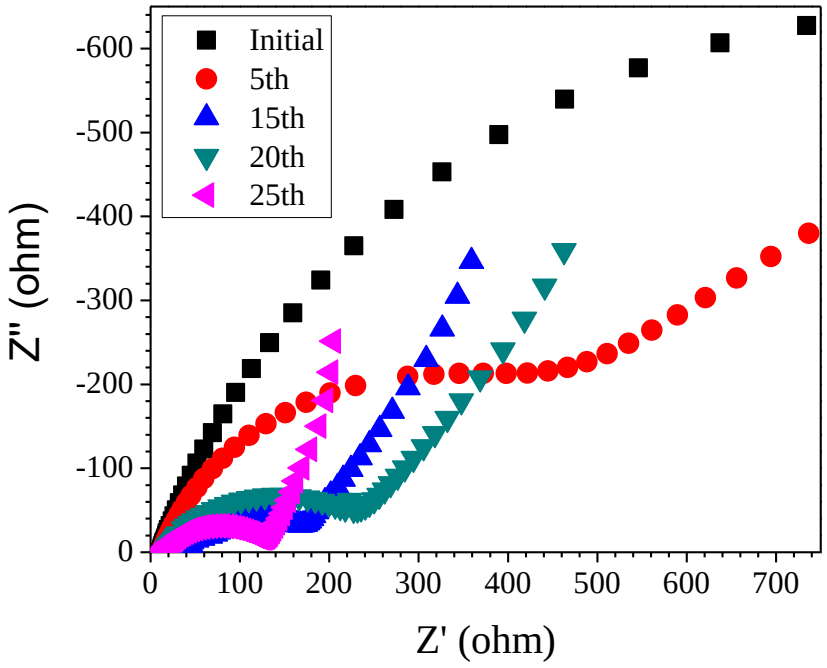

Fig. 5.11. Nyquist plot of a cathode coated graphene sheet.

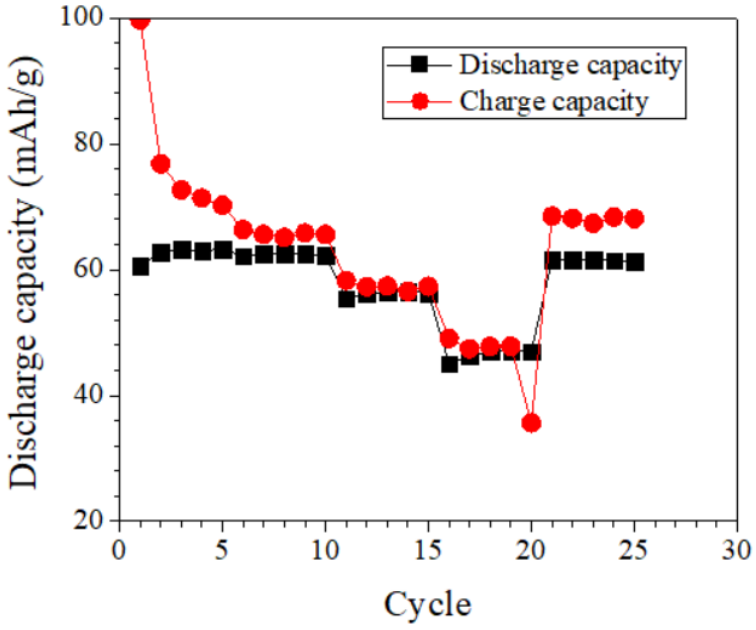

Fig. 5.12. Charge and discharge capacity of a cathode coated with graphene sheet.

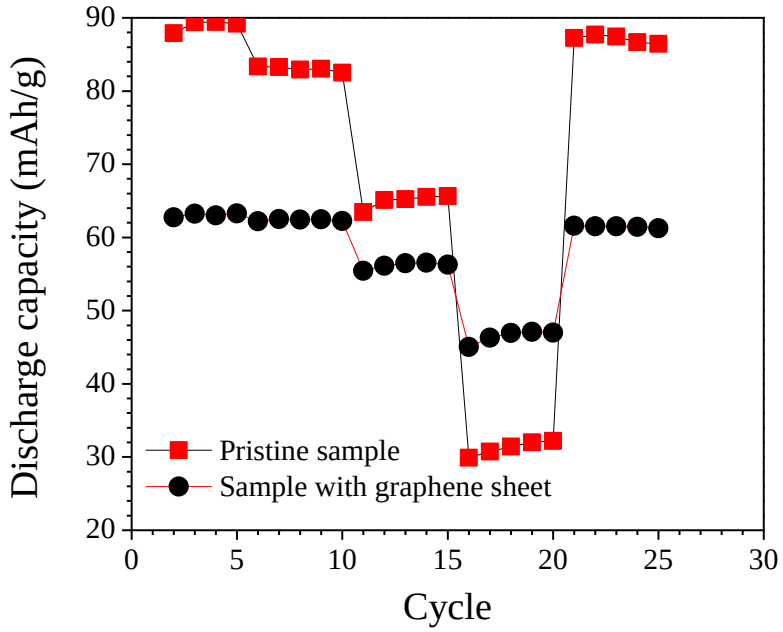

Fig. 5.13. Comparison of discharge capacity between a pristine cathode and cathodes coated with graphene sheet.

However, there are less cathode materials (black part in the Fig. 5.14 (b)) participating in the process of lithium ion transfer due to the graphene sheet coating, which leads to little electrolyte contacting with cathode materials. The cathode materials need to be completely immersed into the electrolyte to drive Li^+ out of the cathode, so there are not many lithium ions going out of the cathode due to the barrier between the cathode and the electrolyte.

In a pristine cathode, there is a SEI film that has a few hundreds of ohms of resistivity and can conduct Li ions. The graphene-sheet coating of high conductivity can prevent the formation of such SEI. However, without SEI, Li ions need to travel distances equivalent to the thickness of the electrodes. So replacing SEI film with graphene sheet has both pros and cons. It could be that at current 2 C, the pros win over the cons. This can explain why cathode has a higher discharge capacity compared with pristine cathode only at 2 C.

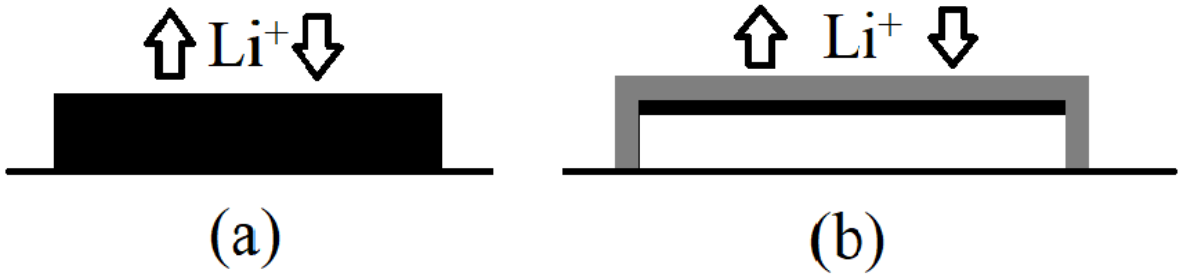

Fig. 5.14. The working mechanism of cathode a) without graphene sheet b) coated graphene sheet.

Chapter 6: Conclusions

One major objective of this research was to test the performance of LIBs using a $LiCoO_2$ cathode incorporated with graphene powder. The results of this work indicate that adding graphene powder into the cathode increases the performance of LIBs. With the incorporation of different weight percentages of graphene powder, the lithium ion cells showed distinct improvement in its charging and discharging characteristics. The cell with 0.5 wt.% graphene powder added to its cathode exhibited the highest discharge capacity at currents 0.1 C and 0.5 C. The incorporation of 1 wt.% graphene powder contributed the most stable performance of the cathode at the currents from 0.1 C to 2 C. The cell with 2 wt.% graphene powder added to its cathode showed an enhanced discharge capacity of the cathode, however, it was less than that of 0.5 wt.% and 1 wt.%.

In order to test the performance of LIBs without a SEI film with a high resistance in this research, one graphene sheet (6-8 layers) was coated on the cathode to impede the formation of SEI layer. The result showed that the incorporation of graphene sheet decreased the discharge capacity of the cathode. In addition, the charge transfer resistance in the electrochemical system increased after coating a graphene film on the cathode. This result can be explained by the transfer limit of Li^+. To avoid formation of SEI film, one graphene sheet was coated on the cathode. However, the graphene sheet blocked the electrolyte immersing into cathode materials, thus, only part of cathode materials participated in the process of lithium ion transfer.

Chapter 7: Improvements and Future Work

7.1 Improvements

Several improvements can be achieved for future research. The process of weighing chemicals can lead to different results. The chemicals were weighed inside the fume hood to prevent environmental effects. However, gentle vibration caused by flowing air inside the fume hood could increase or decrease the actual weights of chemicals. Therefore, a better weighing method is needed.

To ensure consistency of results, more button cells should be assembled and tested. Therefore, the results would be more statistically significant.

7.2 Future Work

The incorporation of graphene powder was shown to enhance the performance of $LiCoO_2$ as a cathode. Different weight percentages of graphene powder were investigated in this research. Future work could focus on adding higher weight percentages (>2 wt.%) of graphene powder into cathode materials to analyze the connection between different weight percentages of graphene powder added and the performance of lithium ion batteries.

References

[1] J. B. Goodenough, “Electrochemical energy storage in sustainable modern society,” Energy and Environmental Science, vol. 7, pp. 14-18, Aug 2014.

[2] Z. G. Yang, J. L. Zhang, M. C. W. Kintner-Meyer, X. C. Lu, D. Choi, J. P. Lemmon, and J. Liu, “Electrochemical energy storage for green grid,” Chemical Reviews, vol. 111, pp. 3577-3613, March 2011.

[3] B. Scrosati, J. Hassoun, and Y. K. Sun, “Lithium-ion batteries. A look into the future,” Energy and Environmental Science, vol. 4, pp. 3287-3295, Sep 2011.

[4] X. Gu, L. Hencz, and S. Q. Zhang, “Recent development of carbonaceous materials for lithium-sulphur batteries,” Batteries, vol. 2, pp. 33, Nov 2016.

[5] G. Kucinskis, G. Bajars, and J. Kleperis, “Graphene in lithium ion battery cathode materials: a review,” Journal of Power Sources, vol. 240, pp. 66-79, April 2013.

[6] J. Zhu, R. Duan, S. Zhang, N. Jiang, Y. Y. Zhang, and J. Zhu, “The application of graphene in lithium ion battery electrode materials,” SpringerPlus, vol. 3, pp. 585, Oct 2014.

[7] N. Kheirabadi and A. Shafiekhani, “Graphene/Li-ion battery,” Journal of Applied Physics, vol. 112, pp. 124323, Dec 2012.

[8] A. K. Geim and K. S. Novoselov, “The rise of graphene,” Nature Materials, vol. 6, pp. 183-191, April 2007.

[9] K. I. Bolotin, K. J. Sikes, Z. Jiang, M. Klima, G. Fudenberg, J. Hone, P. Kim, and H. L. Stormer, “Ultrahigh electron mobility in suspended graphene,” Solide State Communications, vol. 146, pp. 351-355, May 2008.

[10] E. J. Yoo, J. Kim, E. Hosono, H. S. Zhou, T. Kudo, and I. Honma, “Large reversible Li storage of graphene nanosheet families for use in rechargeable lithium ion batteries,” Nano Letters, vol. 8, pp. 2277-2282, July 2008.

[11] G. Wang, B. Wang, X.Wang, J. Park, S. Dou, H. Ahn, and K. Kim, “Sn/graphene nanocomposite with 3D architecture for enhanced reversible lithium storage in lithium ion batteries,” Journal of Materials Chemistry, vol. 19. pp 8378-8384, Oct 2009.

[12] S. Xiong, K. Xie, Y. Diao, and X. Hong, “Characterization of the solid electrolyte interphase on lithium anode for preventing the shuttle mechanism in lithium-sulfur batteries,” Journal of Power Sources, vol. 246, pp. 840-845, Aug 2013.

[13] E. Peled, D. Golodnitsky, and G. Ardel, “Advanced model for solid electrolyte interphase electrodes in liquid and polymer electrolytes,” Journal of The Electrochemical Society, vol. 144, pp. L208-L210, Aug 1997.

[14] E. Peled and S. Menkin, “Review-SEI: past, present and future,” Journal of The Electrochemical Society, vol. 164, pp. A1703-A1719, June 2017.

[15] S. Vazquez, S. M. Lukic, E. Galvan, L. G. Franquelo, and J. M. Carrasco, “Energy storage systems for transport and grid applications,” IEEE Transactions on Industrial Electronics, vol. 57, pp. 3881-3895, Dec 2010.

[16] M. Winter and R. J. Brodd, “What are batteries, fuel cell, and supercapacitors,” Chemical Reviews, vol. 104, pp. 4245-4270, Sep 2004.

[17] A. Yoshino, “The birth of the lithium-ion battery,” Angewandte Chemie International Edition, vol. 51, pp. 5798-800, June 2012.

[18] R. Yazami and P. Touzain, “A reversible graphite-lithium negative electrode for electrochemical generators,” Journal of Power Sources, vol. 9, pp. 365-371, May 1983.

[19] X. Y. Lu, X. H. Jin, and J. Sun, “Adavances of graphene application in electrode materials for lithium ion batteries,” Science China Technological Sciences, vol. 58, pp. 1829-1840, Sep 2015.

[20] S. S. Zhang, R. Jow, K. Amine, and G. L. Henriksen, “$LiPF_6$- EC-EMC electrolyte for Li ion battery,” Journal of Power Sources, vol. 107, pp. 18-23, April 2002.

[21] N. Mahmood and Y. L. Hou, “Electrode nanostructures in lithium-based batteries,” Advanced Science, vol. 1, pp. 1400012, Dec 2014.

[22] Q. Cao, H. P. Zhang, G. J. Wang, Q. Xia, Y. P. Wu, and H. Q. Wu,, “A novel carbon-coated $LiCoO_2$ as cathode material for lithium ion battery,” Electrochemistry Communications, vol. 9, pp. 1228-1232, May 2007.

[23] M. Bryner, “Lithium-ion batteries,” Chemical Engineering Progress, vol. 109, pp. 36, Oct 2013.

[24] M. S. Ding, K. Xu, S. S. Zhang, and T. R. Jow, “Liquid/solid phase diagrams of binary carbonates for lithium batteries part 2,” Journal of The Electrochemical Society, vol. 148, pp. A299-A304, April 2011.

[25] A. Fernicola, B. Scrosati, and H. Ohno, “Potentialities of ionic liquid as new electrolyte media in advanced electrochemical devices,” Ionics, vol. 12, pp. 95-102, July 2006.

[26] C. D. L. Casas and W. Z. Li, “A review of application of carbon nanotubes for lithium ion battery anode material,” Journal of Power Sources, vol. 208, pp. 74-85, June 2012.

[27] M. Z. A. Munshi, Handbook of Solid State Batteries and Capacitors, World Scientific, River Edge, NJ, 1995, pp. 467–512

[28] M. Winter, J. O. Besenhard, M. E. Spahr, and P. Novak, “Insertion electrode materials for rechargeable lithium batteries,” Advanced Materials, vol. 10, pp. 725-763, July 1998.

[29] S. B. Yang, J. P. Huo, H. H. Song, and X. H. Chen, "A comparative study of electrochemical properties of two kinds of carbon nanotubes as anode materials for lithium ion batteris," Electrochimica Acta, vol. 53, pp. 2238-2244, Jan 2008.

[30] C. H. Mi, G. S. Cao, and X. B. Zhao, "A non-GIC mechanism of lithium storage in chemical etched MWNTs" Journal of Electroanalytical Chemistry, vol. 562, pp. 217-221, Feb 2004.

[31] K. Nishidate and M. Hasegawa, "Energetics of lithium ion adsorption on defective carbon nanotubes," Physical Review B, vol. 71, pp. 245418, June 2005.

[32] V. Meunier, J. Kephart, C. Roland, and J. Bernholc, "Ab initio investigations of lithium diffusion in carbon nanotube systems," Physical Review Letters, vol. 88, pp. 075506, Feb 2002.

[33] M. M. Atabaki and R. Kovacevic, "Graphene composites as anode materials in lithium-ion batteries," Electronic Materials Letters, vol. 9, pp. 133-153, March 2013.

[34] G. Amatucci and J. M. Tarascon, "Optimization of insertion compounds such as $LiMn_2O_4$ for Li-ion batteries," Journal of the electrochemical society, vol 149, pp. 31-46, Nov 2002.

[35] S. M. Bak, K. W. Nam, C. M. Lee, K. H. Kim, H. C. Jung, X. Q. Yang, and K. B. Kim, "Spinel $LiMn_2O_4$ reduced graphene oxide hybrid for high rate lithium ion batteries," Journal of Materials Chemistry, vol. 21, pp. 17309-17315, Oct 2011.

[36] M. Goosey, "A short introduction to graphene and its potential interconnect applications," Circuit World, vol. 38, pp. 83-86, 2012.

[37] D. D. L. Chung, "Review graphite," Journal of Materials Science, vol. 37, pp. 1475-1489, April 2002.

[38] K. S. Novoselov, A. K. Geim, S. V. Morozov, D. Jiang, Y. Zhang, S. V. Dubonos, I. V. Grigorieva, and A. A. Firsov, "Electric field effect in atomically thin carbon films," Science, vol. 306, pp. 666-669, Oct 2004.

[39] M. D. Stoller, S. Park, Y. W. Zhu, J. H. Ao, and R. S. Ruoff, "Graphene-based ultracapacitors," Nano Letters, vol. 8, pp. 3498-3502, Sep 2008.

[40] S. R. C. Vivekchand, C. S. Rout, K. S. Subrahmanyam, A. Govindaraj, and C. N. R. Rao, "Graphene-based electrochemical supercapacitors," Journal of Chemical Sciences, vol. 120, pp. 9-13, Jan 2008.

[41] B. Partoens and F. M. Peeters, "From graphene to graphite: electronic structure around the K point," Physical Review B, vol. 74, pp.075404, August 2006.

[42] G. Jo, M. Choe, S, Lee, W. Park, Y. H. Kahng, and T. Lee, “The application of graphene as electrodes in electrical and optical devices,” Nanotechnology, vol. 23, pp. 112001, Feb 2012.

[43] K. V. Emtsev, F. Speck, T. Seyller, L. Ley, and J. D. Riley, “Interaction, growth, and ordering of epitaxial graphene on SiC{0001} surface: A comparative photoelectron spectroscopy study,” Physical Review B, vol. 77, pp. 155303, April 2008.

[44] V. C. Tung, M. J. Allen, Y. Yang, and R. B. Kaner, “High-throughput solution processing of large-scale graphene,” Nature Nanotechnology, vol. 4, pp. 25-29, Nov 2008.

[45] S. Bae, H. Kim, Y. Lee, X. Xu, J. Park, Y. Zheng, J. Balakrishnan, T. Lei, H. R. Kim, Y. Song, Y. J. Kim, K. S. Kim, B. Ozyilmaz, J. H. Ahn, B. H. Hong, and S. Iijima, “Roll-to-roll production of 30-inch graphene films for transparent electrodes,” Nature Nanotechnology, vol. 5, pp. 574-578, June 2010.

[46] J. P. Zhu, W. Zu, G. Yang, and Q. F. Song, “A novel electrochemical supercapacitor based on $Li_4Ti_5O_{12}$ and $LiNi_{1/3}Co_{1/3}Mn_{1/3}O_2$,” Materials Letters, vol. 15, pp. 237-240, Jan 2014.

[47] P. Simon and Y. Goqotsi, “Materials for electrochemical capacitors,” Nature Materials, vol. 7, pp. 845-54, Nov 2008.

[48] S. Z. Liang, X. F. Zhu, P. C. Lian, W. S. Yang, and H. H. Wang, “Superior cycle performance of Sn@C/graphene nanocomposites as an anode material for lithium-ion batteries,” Journal of Solid State Chemistry, vol. 184, pp. 1400-1404, June 2011.

[49] M. V. Reddy, G. V. S. Rao, and B. V. R. Chowdari, “Metal oxides and oxysalts as anode materials for Li ion batteries,” Chemical Reviews, vol. 113, pp. 5364-5457, April 2013.

[50] J. Wolfenstine, “Critical grain size for microcracking during lithium insertion,” Journal of Power Sources, vol. 79, pp. 111-113, May 1999.

[51] V. Manev, B. Banov, A. Momchilov, and A. Nassalevska, “$LiMn_2O_4$ for 4V lithium-ion batteries,” Journal of Power Sources, vol. 57, pp. 99-103, Dec 1995.

[52] J. M. Tarascon and D. Guyomard, “The $Li_{1+x}Mn_2O_4$/C rocking-chair system: a review,” Electrochimica Acta, vol. 38, pp. 1221-1231, June 1993.

[53] X. Zhao, C. M. Hayner, and H. H. Kung, “Self-assembled lithium manganese oxide nanoparticles on carbon nanotube or graphene as high-performance cathode material for lithium-ion batteries,” Journal of Materials Chemistry, vol. 21, pp. 17297-17303, Sep 2011.

[54] S. J. R. Prabakar, Y. H. Hwang, B. Lee, K. S. Sohn, and M. Pyo, “Graphene-sandwiched $LiNi_{0.5}Mn1.{}_5O_4$ cathode composites for enhanced high voltage performance in Li ion

batteries," Journal of The Electrochemical Society, vol. 160, pp. A832-A837, March 2013.

[55] R. Amin and J. Maier, "Effect of annealing on transport properties of $LiFePO_4$: Towards a defect chemical model," Solid State Ionics, vol. 178, pp. 1831-1836, Feb 2008.

[56] C. Su, X. D. Bu, L. H. Xu, J. L. Liu, and C. Zhang, "A novel $LiFePO_4$/graphene/carbon composite as a performance-improved cathode material for lithium-ion batteries," Electrochimica Acta, vol. 64, pp. 190-195, March 2012.

[57] Y. Ding, Y. Jiang, F. Xu, J. Yin, H. Ren, Q. Zhuo, Z. Long, and P. Zhang, "Preparation of nano-structured $LiFePO_4$/graphene composites by co-precipitation method," Electrochemistry Communications, vol. 12, pp. 10-13, Jan 2010.

[58] H. Xu, J. Chang, J. Sun, and L. Gao, "Graphene-encapsulated LiFePO4 nanoparticles with high electrochemical performance for lithium ion batteries," Materials Letters, vol. 83, pp. 27-30, Sep 2012.

[59] X. F. Zhou, F. Wang, T. M. Zhu, and Z. P. Liu, "Graphene modified $LiFePO_4$ cathode materials for high power lithium ion batteries," Journal of Materials Chemistry, vol. 21, pp. 3353-3358, Jan 2011.

[60] W. M. Chen, L. Qie, L. X. Yuan, S. A. Xia, X. L. Hu, W. X. Zhang, and Y. H. Huang, "Insight into the improvement of rate capability and cyclability in $LiFePO_4$/polyaniline composite cathode," Electrochimica Acta, vol. 56, pp. 2589-2695, Feb 2011.

[61] O. Toprakci, H. A. K. Toprakci, L. W. Ji, G. J. Xu, Z. Lin, and X. W. Zhang, "Carbon nanotube-loaded electrospun LiFePO4/carbon composite nanofibers as stable and binder-free cathodes for rechargeable lithium-ion batteries," ACS Applied Materials and Interfaces, vol. 4, pp. 1273-1280, Feb 2012.

[62] H. Huang, T. Faulkner, J. Barker, and M. Y. Saidi, "Lithium metal phosphates, power and automotive applications," Journal of Power Sources, vol. 189, pp. 748-751, April 2009.

[63] F. Yu, J. J. Zhang, Y. F. Yang, and G. Z. Song, "Preparation and electrochemical performance of $Li_3V_2(PO_4)_3$/C cathode material by spraying-drying and carbothermal method," Journal of Solid State Electrochemistry, vol. 14, pp. 883-888, May 2010.

[64] H. D. Liu, P. Bao, J. H. Fang, and G. Yang, "$Li_3V_2(PO_4)_3$/graphene nanocomposites as cathode material for lithium ion batteries," Chemical Communications, vol. 47, pp. 9110-9112, July 2011.

[65] Sigma-Aldrich, 2033 Westport Center Dr, St. Louis, MO 63146. https://www.sigmaaldrich.com/united-states.html.

[66] Alfa Aesar, 2 Radcliff Rd Tewksbury, MA 01876. https://www.alfa.com/en/

[67] Graphene Supermarket, 4603 Middle Country Rd Unit 125 Calverton, NY, 11933. https://graphene-supermarket.com/

[68] ACS Material, 959 E Walnut Street Unit 100, Pasadena, CA 91106. https://www.acsmaterial.com/

[69] B. Peng, Y. Xu, X. Wang, X. Shi, and F. M. Mulder, "The electrochemical performance of super P carbon black in reversible Li/Na ion uptake," Science China Physics, vol. 60, pp. 064611, June 2017.

[70] R. Dominko, M. Gaberscek, J. Drofenik, M. Bele, and S. Pejovink, "A novel coating technology for preparation of cathodes in Li-ion batteries," Electrochemical and Solid-State Letters, vol. 4, pp. A187-A190, Sep 2001.

[71] R. Dominko, M. Gaberscek, J. Drofenik, M. Bele, S. Pejovnik, and J. Jamnika, "The role of carbon black distribution in cathodes for Li ion batteries," Journal of Power Sources, vol 119-121, pp. 770-773, June 2003.

[72] Y. L. Li, B. W. Xiao, D. S. Geng, and X. L. Sun, "Carbon black cathodes for lithium oxygen batteries: Influence of porosity and heteroatom-doping," Carbon, vol. 64, pp. 170-177, Nov 2013.

[73] R. M. Gnanamuthu and C. W. Lee, "Electrochemical properties of super p carbon black as an anode active material for lithium-ion batteries," Materials Chemistry and Physics, vol. 130, pp. 831-834, Nov 2011.

[74] J. Kim, B. Kim, J. G. Lee, J. Cho, and B. Park, "Direct carbon-black coating on $LiCoO_2$ cathode using surfactant for high-density Li-ion cell," Journal of Power Sources, vol. 139, pp. 289-294, Sep 2004.

[75] K. Krizek, J. Ruzicka, M. Julinova, L. Husarova, J. Houser, M. Dvorackova, and P. Jancova, "N-methyl-2-pyrrolidone-degrading bacteria from activated sludge," Water Science and Technology, vol. 71, pp/ 776-82, March 2015.

[76] V. V. Panic, R. M. Stevanovic, V. M. Jovanovic, and A. B. Dekanski, "Electrochemical and capacitive properties of thin-layer carbon black electrodes," Journal of Power Sources, vol. 181, pp. 186-192, June 2008.

[77] C. Daniel, "Materials and processing for lithium-ion batteries," The Journal of The Minerals, Metals and Materials Society, vol. 60, pp. 43-48, Sep 2008.

[78] Z. Zhang, T. Zeng, Y. Lai, M. Jia, and J. Li, "A comparative study of different binders and their effects on electrochemical properties of $LiMn_2O_4$ cathode in lithium ion batteries," Journal of Power Sources, vol. 247, pp. 1-8, Feb 2014.

[79] P. Arora and Z. Zhang, "Battery separators," Chemical Reviews, vol. 104, pp. 4419-4462, Oct 2004.

[80] X. Huang and J. Hitt, “Lithium ion battery separators: Development and performance characterization of a composite membrane,” Journal of Membrane Science, vol. 425-426, pp. 163-168, Jan 2013.

[81] H. Lee, M. Yanilmaz, O. Toprakci, K. Fu, and X. Zhang, “A review of recent development in membrane separators for rechargeable lithium-ion batteries,” Energy and Environmental Science, vol 7, pp. 3857-3886, Aug 2014.

[82] R. E. Sousa, J. N. Pereira, C. M. Costa, M. M. Silva, S. L. Mendz, J. Hassoun, B. Scrosati, and G. B. Appetecchi, “Influence of the porosity degree of poly(vinylidene fluoride-co-hexafluoropropylene) separators in the performance of Li-ion batteries,” Journal of Power Sources, vol. 263, pp. 29-36, Oct 2014.

[83] F. Croce, M. L. Focarete, J. Hassoun, I. Meschini, and B. Scrosati, “A safe, high-rate and high-energy polymer lithium-ion battery based on gelled membranes prepared by electrospinning,” Energy and Environmental Science, vol. 4, pp. 921-927, March 2011.

[84] K. Omote and H. Ohigashi, “Temperature dependence of elastic, dielectric, and piezoelectric properties of “single crystalline” films of vinylidene fluoride trifluoroethylene copolumer,” Journal of Applied Physics, vol. 81, pp. 2760, Aug 1998.

[85] Z. Liu, H. Zhou, S. S. Ang, and J. Zhang, “Evaluation of low-cost natrochalcite $Na[Cu_2(OH)(H_2O)(SO_4)_2]$ as an anode material for Li- and Na-ion batteries,” Electrochimica Acta, vol. 211, pp. 619-626, Sep 2016.

[86] VWR, 100 Matsonford Road, Radnor, PA 19087. https://www.vwr.com/contact_us.htm.

[87] Branson, 41 Eagle Road Danbury, CT 06810. https://www.bransonic.com/.

[88] PHI, 14955 Salt Lake Ave. City of Industry, CA 91746. http://phihydraulics.com/.

[89] Mbraun, 14 Marin Way Stratham, NH 03885. http://www.mbraun.com/index.php.

[90] Celgard, 13800 South Lake Dr. Charlotte, NC 28273. https://www.celgard.com/.

[91] CH Instruments, Inc., 3700 Tennison Hill Drive, Austin TX 79738. http://www.chinstruments.com/.

[92] Arbin Instruments, 762 Peach Creek Cut Off Rd. College Station, TX 77845. http://www.arbin.com/.

[93] S. M. Park and J. S. Yoo, “Electrochemical impedance spectroscopy for better electrochemical measurements,” Analytical Chemistry, vol. 75, pp. 455A-461A, Nov 2003.

[94] A. Amirudin and D. Thierry, “Application of electrochemical impedance spectroscopy to study the degradation of polymer-coated metals,” Progress in Organic Coating, vol. 26, pp. 1-28, May 1995.

[95] Z. He and F. Mansfeld, “Exploring the use of electrochemical impedance sepectroscopy (EIS) in microbial fuel cell studies,” Energy and Environmental Science, vol. 2, pp. 215-219, Nov 2008.

[96] B. L. Corso, I. Perez, T. Sheps, P. C. Soms, O. T. Gul, and P. G. Colloins, “Electrochemical charge-transfer resistance in carbon nanotube composites,” Nano Letters, vol. 14, pp. 1329-1336, Feb 2014.

[97] B. Y. Chang and S. M. Park, “Electrochemical impedance spectroscopy,” Annual Reviews, vol. 3, pp. 207-29, Feb 2010.

[98] R. Tang, Q. Yun, W. Lv, T. He, C. You, F. Su, L. Ke, B. Li, F. Kang, and Q. Yang, “How a very trace amount of graphene additive works for constructing an efficient network in $LiCoO_2$-based lithium-ion batteries,” Carbon, vol. 103, pp. 356-362, July 2016.

[99] H. Wang, Y. Yang, Y. Liang, L. Cui, H. S. Casalongue, Y. Li, G. Hong, Y. Cui, and H. Dai, “$LiMn_{1-x}Fe_xPO_4$ nanorods grown on graphene sheets for ultrahigh-rate-performance lithium ion batteries,” Angewandte Chemie International Edition, vol. 50, pp. 7364-7368, June 2011.

Appendix A: Description of Research for Popular Publication

How a better lithium ion battery influence human life.

Nowadays, lithium ion batteries (LIBs) are widely used for cell phones, laptops, and electric vehicles (EVs). They are playing essential roles in the current society. However, LIBs cannot satisfy the requirements from customers. For example, there are many complaints that cell phones need to be frequently charged in one day. Electric vehicles is another potential field which leads to a new future. However, electric vehicles are not a proper option for a long distance trip due to the low electrical capacity of their batteries. Therefore, batteries need to be improved and have more capacity, or it could be lighter or smaller with a given capacity. There is another direction, which is to find a new battery to replace the dominating lithium ion batteries.

Graphene is always an attractive topic since it was discovered. It is widely used in the field of LIBs, fuel cells, and supercapacitors. One of many advantages of graphene is its significant electrical conductivity. There are many papers reporting the applications of graphene into different anode and cathode materials. These papers indicate that the incorporation of graphene into cathode or anode materials improves the performance of batteries. However, there are no papers published indicating the result of $LiCoO_2$/graphene (0.5 wt.% and 1 wt.%) composite as a cathode.

In this research, graphene powder and graphene sheet were incorporated into $LiCoO_2$ as a cathode. The cathode materials also included carbon black, NMP, PVDF, which are common electrode materials. EIS measurement can explore the electrochemical behavior of a cell. The charge transfer resistance could be indicated from EIS measurements. A low charge transfer resistance was an objective of this work. Several parameters, such as charge and discharge

capacity, voltage, can be obtained from full cycles of charging and discharging. A higher discharge capacity value was another objective in this research.

As a result, all cells incorporated with graphene powder had increased discharge capacity. The cathodes incorporated with 0.5 wt.% graphene powder showed the highest discharge capacity at the current 0.1 C and 0.5 C. 1 C is the current that can fully charge and discharge a cell in one hour. The incorporation of 1 wt.% graphene powder offers the most stable performance of the cell. The cells with their cathodes having 2 wt.% graphene powder added have an increased discharge capacity. The cathodes coated with a graphene sheet show a lower discharge capacity compared with pristine cathode. This can be caused by the graphene sheet impeding the transfer of lithium ions.

Appendix B: Summary of Newly Created Intellectual Property

The following list of new intellectual property items were created in the course of this research project and should be considered from both a patent and commercialization perspective.

1. The performance of cathodes ($LiCoO_2$: PVDF: Carbon Black = 80 wt.%: 10 wt.%: 10 wt.%) with the incorporation of graphene powder (0.5 wt.%, 1 wt.%, and 2 wt.%) were tested.
2. The performance of cathodes coated with an unbroken graphene sheet (6-8 layers) was tested.

Appendix C: Potential Patent and Commercialization Aspects of listed Intellectual Property Items

C.1 Patentability of Intellectual Property (Could Each Item be Patented)

The two items listed were considered first from the perspective of whether or not the item could be patented.

1. The incorporation of graphene powder into $LiCoO_2$ could not be patented, because there are already many papers reporting the incorporation of graphene powder into $LiCoO_2$.
2. The incorporation of graphene sheet into $LiCoO_2$ could be patented since no one has previously coated an integrated graphene sheet on the surface of the cathode.

C.2 Commercialization Prospects (Should Each Item Be Patented)

The two items listed were then considered from the perspective of whether or not the item should be patented.

1. The incorporation of different weight percentages (0.5 wt.%, 1 wt.%, and 2 wt.%) graphene powder could not be patented, because many researchers have done the incorporation of graphene powder into $LiCoO_2$.
2. The incorporation of graphene sheet should not be commercialized because it did not provide an increased discharge capacity to each sample.

C.3 Possible Prior Disclosure of IP

The following item was discussed in a public forum or have published information that could impact the patentability of the listed IP.

1. This research and thesis content have not been publicly unclosed.

Appendix D: Broader Impact of Research

D.1 Applicability of Research Methods to Other Problems

The investigations of adding graphene into electrode materials are extremely common in the research of lithium ion batteries. The method of incorporating graphene could be used as a method to add other electrode additives, such as graphene foam, or adding graphene to other electrode materials, such as $LiFePO_4$.

D.2 Impact of Research Results on U.S. and Global Society

With a higher discharge capacity, lithium ion batteries will retain its dominant application. Cell phones and laptops are playing essential roles in daily life. Lithium ion batteries with an increased capacity will allow portable devices to be used for a longer time without charging. Therefore, it could improve the efficiency of working and living for all humans.

The electric vehicle is becoming more and more popular all over the world. Companies, such as Tesla and Toyota, are putting much effort into the investigation of EVs. With a higher capacity of electrical energy, EVs can run for a longer distance with only one charge making their use more economically viable.

D.3 Impact of Research Results on the Environment

Modern society consumes tons of batteries every day and countless exhausted batteries are discarded. With a higher discharge capacity, lithium ion batteries can be used for a longer time, which leads to fewer batteries discarded. Therefore, less pollution from lithium ion batteries will be achieved. With a longer lifespan, batteries do not need to be replaced as frequently.

In addition, more EVs and HEVs would be used due to longer distance achievable by the larger electrical energy capacity. The current society consumes tremendous fossil fuel energy which leads to serious environmental issues such as global warming. In addition, automobile exhaust from combustion engines cause severe air pollution. With the use of EVs and HEVs, the environment will be subjected to less pollution.

Appendix E: Microsoft Project for MS MicroEP Degree Plan

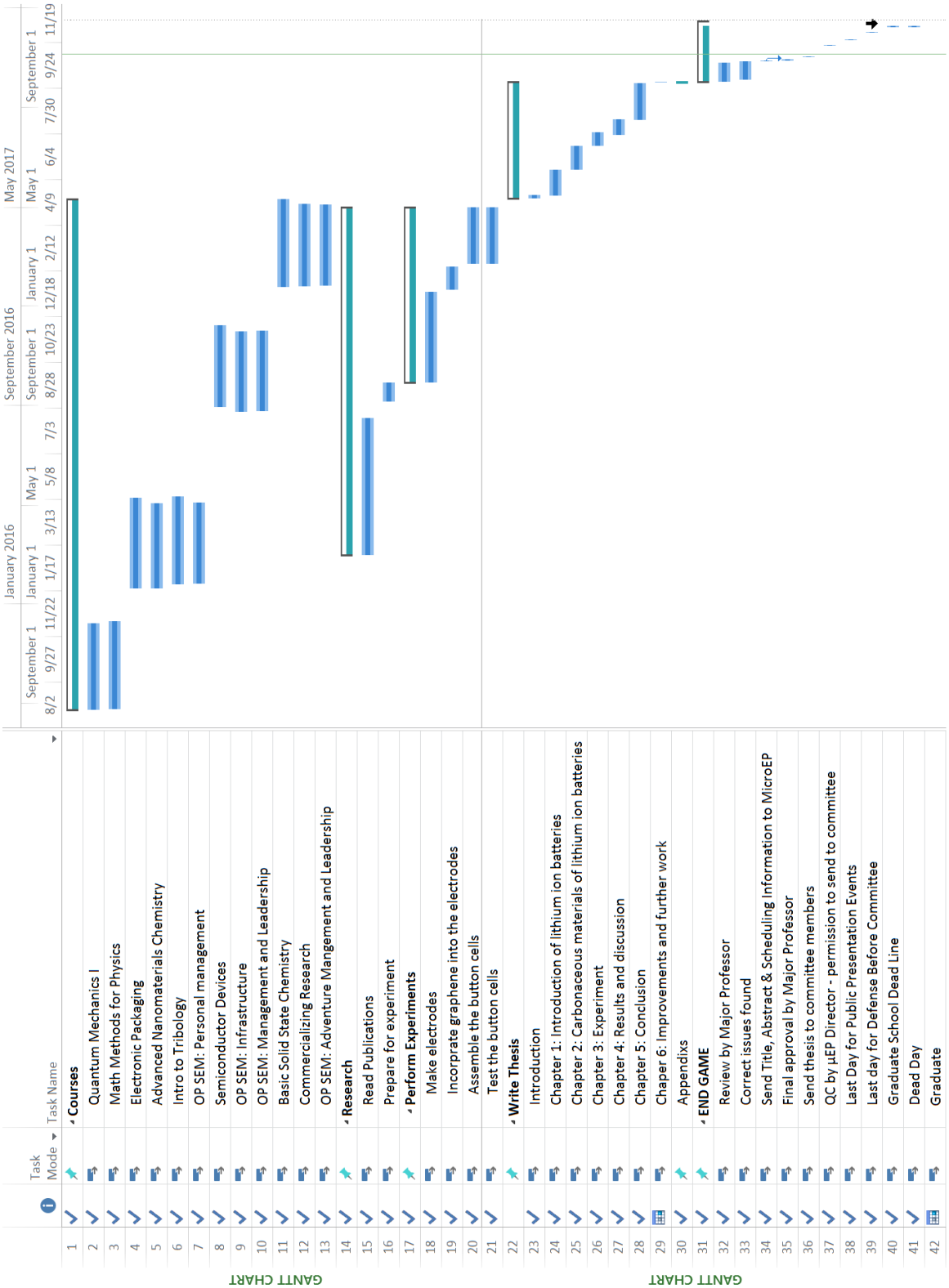

Appendix F: Identification of All Software Used in Research and Thesis Generation

Computer #1:

Model Number: Dell Dimension 8300

Location: ENRC 4267

Owner: Prof. Simon S. Ang

Software #1:

Name: CHI660D

Purchased by: Prof. Simon S. Ang

Software #2:

Name: Battery Analyzer Program

Purchased by: Prof. Simon S. Ang

Computer #2:

Model Number: Dell Inspiron 13

Location: 2100 N Leveret Ave Apt 130

Owner: Kenan Wang

Software #1:

Name: Microsoft Program

Purchased by: Kenan Wang

Software #2:

Name: OriginPro 8

Purchased by: Kenan Wang

Appendix G: All Publications Published, Submitted and Planned

Planned:

1. Kenan Wang, Huajun Zhou, and Simon Ang, "The incorporation of graphene into $LiCoO_2$ as a cathode to improve the performance of LIBs," (to be submitted to the Journal of Power Sources).